Advanced organic nanocomposite coatings for effective corrosion protection

Samarah Vargas Harb, Andressa Trentin,
Mayara Carla Uvida, Peter Hammer

São Paulo State University (UNESP), Institute of Chemistry, Araraquara, SP, Brazil

1. Introduction

Polymeric materials have transformed our daily lives due to their broad applicability, ranging from household appliances to aircraft components. Tailoring polymer architecture, chain length, monomer arrangement in copolymers, tacticity, 3D cross-linking, and crystallinity, among other features, polymers can be designed for specific applications. Besides the diversity of polymeric structures, the incorporation of additives such as clays, lignin, collagen, hydroxyapatite, chitosan, carbon nanostructures, organic and inorganic corrosion inhibitors, metallic or ceramic nanoparticles can further improve their functionality in terms of thermal stability, mechanical strength, fire retardancy, corrosion resistance, gas barrier property, self-healing ability, bioactivity, or other desired characteristics.

In the field of corrosion protection, coatings based on polymeric nanocomposites are of great interest due to the mild synthesis conditions, processability, simple deposition, low cost, and principally due to their outstanding anticorrosive performance [1]. Acrylate, epoxy, and polyurethane-based coatings are the most widely applied polymeric materials for corrosion protection of metallic surfaces; however, different other polymeric matrices have already been tested, including fluoropolymers, conducting polymers, and polyesters.
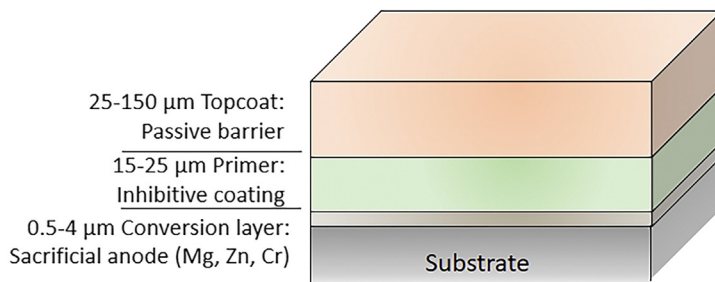
The most commonly used corrosion protection strategy for steel and aluminum is based on protective multi-layer coatings by applying first a 0.5−4.0 μm thick layer composed by sacrificial anodes (Mg and Zn), chromating of galvanized surfaces, and phosphating or anodizing of aluminum; a second layer, named primer, with a thickness of 15−25 μm, based on epoxy resin loaded with curing agent and corrosion inhibitors (phosphate, zinc, cerium,

benzotriazole, etc.), which is responsible for the adhesion to the pretreated surface; and finally, a third layer with a thickness of 25—150 μm, called topcoat, provides a passive barrier protection against the permeation of corrosive species (Fig. 17.1) [2]. Epoxy resins are the mostly applied primers and topcoats, offering excellent results in terms of corrosion protection. Concerning this approach, however, there are several critical issues to be noted: (1) the use of toxic species to produce conversion layers, such as hexavalent chromium, (2) poor adhesion of polymeric paints to the metallic substrate, which often leads to coating detachment and failure, (3) relatively low thermal stability of polymeric materials, and (4) high costs associated with the complex deposition process and amount of necessary materials.

Several recent studies have shown the possibility of replacing the established corrosion protection strategy by polymeric nanocomposites, which offer very effective protection using only a thin (1—10 μm) single layer. In this context, especially organic—inorganic nanocomposites based on poly(methyl methacrylate) (PMMA)—silica and epoxy—silica hybrids applied directly on bare metallic surface have presented notable corrosion protection efficiency and durability. The presence of the inorganic phase improves the coating adhesion by covalent linking to the substrate and stabilizes by cross-linking the polymeric phase, which in turn provides a crack- and pore-free matrix, resulting in an efficient anticorrosion barrier [1]. It is important to stress the crucial role of the hybrid interphase that in the form of a coupling molecule provides covalent bonding between both phases. This linking leads to a contraction of the polymer chain segments, inhibiting material swelling and consequently improving the blocking character of the coating [1].

Anticorrosion coatings are mainly characterized using electrochemical impedance spectroscopy (EIS) and potentiometric polarization curves to assess their corrosion resistance and stability after salt spray test or immersion in aggressive solutions. However, a number of other techniques focusing on structural properties (Raman, infrared [FTIR], X-ray photoelectron [XPS], X-ray absorption, secondary ion mass spectroscopies, nuclear magnetic resonance, small angle X-ray scattering), morphology (atomic force, scanning electron , and transmission electron microscopies), thermal stability (thermogravimetry, differential scanning calorimetry), and mechanical characteristics (microscratch, nanoindentation, adhesion) are applied to elucidate, in more detail, their barrier properties. The aim of this chapter is to give an overview of several classes of polymeric nanocomposites used for corrosion protection and to relate their structural properties with anticorrosive efficiency.

FIGURE 17.1 State-of-the-art strategy for corrosion protection coatings.

25-150 μm Topcoat: Passive barrier

15-25 μm Primer: Inhibitive coating

0.5-4 μm Conversion layer: Sacrificial anode (Mg, Zn, Cr)

Substrate

2. Acrylate-based nanocomposites

Acrylates, also known as acrylics or polyacrylates, represent a group of thermoplastic polymers that are widely used due to their transparency and resistance under aggressive environmental conditions. They comprise polymers obtained from a large number of monomers, such as acrylic acid, methyl methacrylate (MMA), methyl acrylate, ethyl acrylate, 2-ethylhexyl acrylate, 2-hydroxyethyl methacrylate (HEMA), and glycidyl methacrylate, among others (Fig. 17.2). The excellent corrosion protection results achieved using acrylate coatings on different metallic substrates have inspired several research groups to combine this variety of polymers with different classes of nanofillers. This integration, when properly accomplished, enables to produce low-thickness coating with high anticorrosive performance at low costs [1].

For the synthesis of acrylates, the organic monomer is polymerized in three steps (initiation, propagation, and termination) through an anionic, cationic, thermal or photo initiator of polymerization using ultraviolet light [3,4]. The most commonly used thermal initiation occurs by the polymerization of carbon—carbon (vinyl) double bonds via radical initiation under heating using benzoyl peroxide or azobisisobutyronitrile [5,6], as represented in Fig. 17.3. Peroxides and azo-compounds can undergo hemolytic cleavage rather easily by heating and breaking the oxygen—oxygen bond and nitrogen—carbon bond, respectively. The radical synthesized polymers have an average molar mass that depends on the temperature and the concentration of the initiator, thus allowing to control the final structure [6].

Although resistant to hydrolysis and ultraviolet radiation during prolonged weathering, pure acrylic systems present limitations, including poor thermal stability and mechanical resistance, swelling of polymeric chains on immersion, and poor adhesion to the substrate due to the absence of covalent bonds at the interface [1,7]. These drawbacks can be overcome by the incorporation of inorganic nanophases in the polymer matrix such as CeO_2 [8], ZnO [9], and SiO_2 [10]. With the addition of inorganic nanoparticles into the polymeric network, the interstitial voids are filled, and covalent bonds may be formed at the organic—inorganic interphase and at the metal/coating interface, thus improving the corrosion resistance and durability of the coatings.
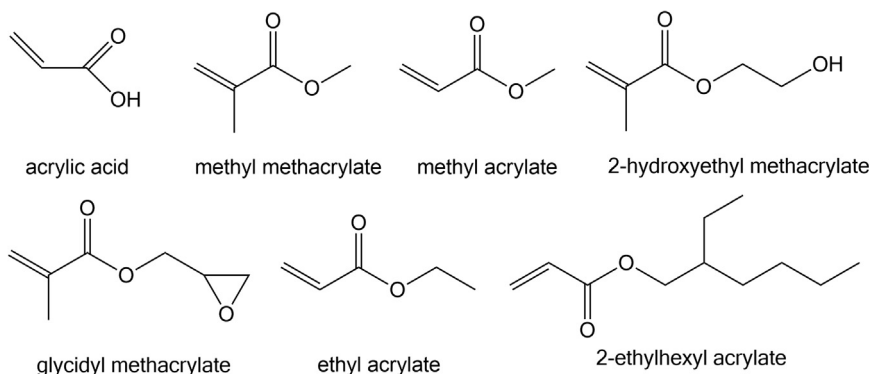

FIGURE 17.2   Molecular structure of monomers of acrylic nanocomposites.

FIGURE 17.3 Hemolytic cleavage of the
thermal initiators: (A) benzoyl peroxide and
(B) azobisisobutyronitrile. (C) Free radical poly-
merization of methyl methacrylate. *Adapted from
K. van Rijswijk, H.E.N. Bersee, Reactive processing of
textile fiber-reinforced thermoplastic composites — an
overview, Compos. Part A Appl. Sci. Manuf. 38
(2007) 666–681 and C. Duval-Terrié, L. Lebrun,
Polymerization and characterization of PMMA, J.
Chem. Educ. 2 (2006) 443–446.*
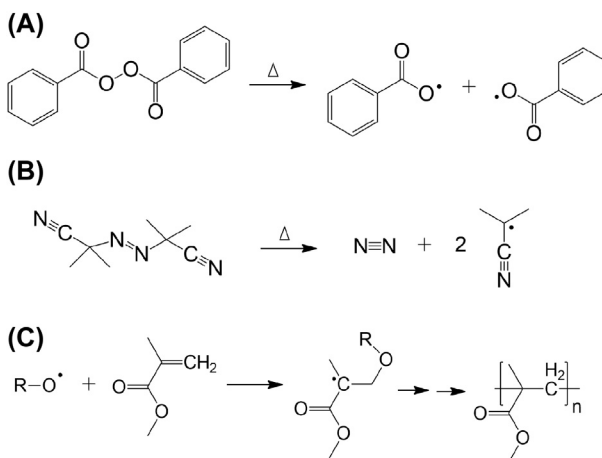
To achieve adequate homogenization during the formation of nanocomposites, a series of synthesis parameters must be optimized, in particular the interaction between the acrylic monomers and the inorganic additives. For this purpose, coupling molecules — containing an inorganic group attached to an acrylic tail — have been used to establish covalent linking between both phases, thus creating cross-linking nodes that densify the structure by contracting the polymer chain segments [11]. Some examples for coupling agents composed of acrylate monomers linked to silane or hydroxyl functional groups include 3-(trimethoxysilyl) propyl methacrylate (MPTS), 3-(trimethoxysilyl)propylacrylate, vinyl triethoxysilane, vinyl-trimethoxysilane, and HEMA, among others (Fig. 17.4). These molecules are able to prevent the aggregation of inorganic particles by linking to the polymeric phase and to provide improved adhesion to metallic substrates by forming covalent bonds between the silanol groups and terminal hydroxyl bonds of the metal surface [7,11]. The use of coupling agents has yielded remarkable improvement of the protective performance of the coatings without affecting the hybrid structure, thanks to the functional similarity with both phases [12,13].

The integration of inorganic nanophases in an acrylic polymer matrix has proved to be very promising for the design of high-performance hybrid coatings and therefore has been the subject of a detailed study by varying parameters such as type and proportion of precursor reagents, reaction time, temperature, solvent, and type of substrate [1,10,14]. Recent advances achieved for acrylic nanocomposite coatings in terms of low electrolyte permeation, strong adhesion to the substrate, thermal stability, mechanical strength, and especially high durability in aggressive environments make them a potential alternative to conventional coating systems used in the automotive and aeronautic industry, construction, offshore installations, etc.

Considering the protection efficiency of carbon steel, extensively used in the automotive industry and construction, interesting results have been reported for the PMMA system covalently bonded to silica nanoparticles. This is achieved by combining the polymerization process of MMA monomers with the sol–gel route of hydrolytic condensation of the silicon alkoxide precursor including a suitable coupling agent [12,15]. Using this approach under
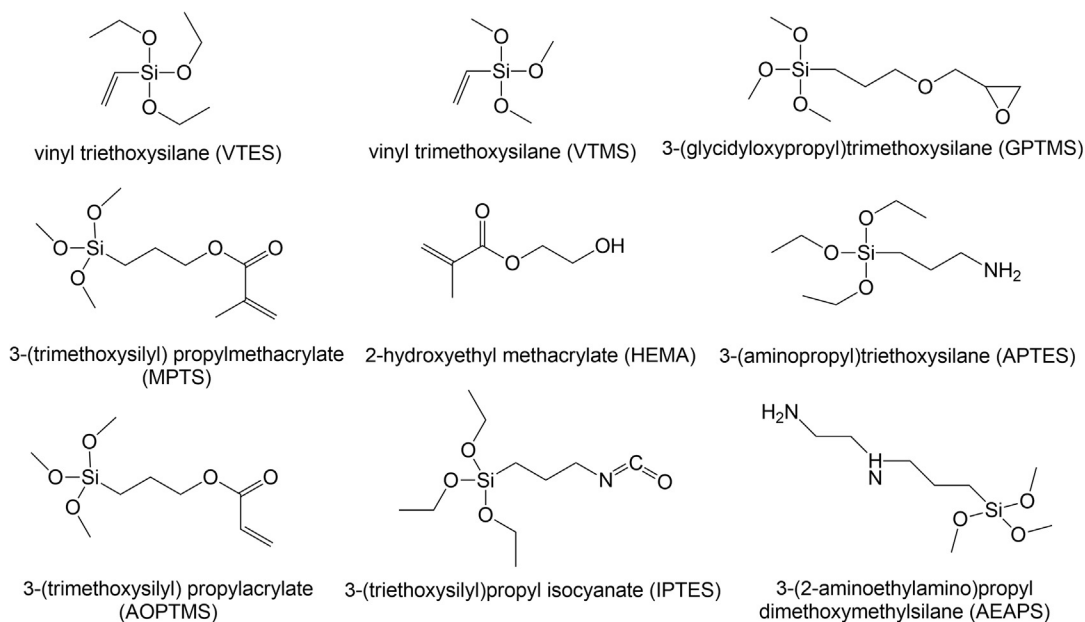
vinyl triethoxysilane (VTES)   vinyl trimethoxysilane (VTMS)   3-(glycidyloxypropyl)trimethoxysilane (GPTMS)

3-(trimethoxysilyl) propylmethacrylate (MPTS)   2-hydroxyethyl methacrylate (HEMA)   3-(aminopropyl)triethoxysilane (APTES)

3-(trimethoxysilyl) propylacrylate (AOPTMS)   3-(triethoxysilyl)propyl isocyanate (IPTES)   3-(2-aminoethylamino)propyl dimethoxymethylsilane (AEAPS)

FIGURE 17.4   Molecular structure of most commonly used organic—inorganic coupling agents.

variation of the MMA to MPTS molar ratio in the organic phase, Hammer et al. have reported PMMA—silica coatings with a high corrosion resistance, maintaining the low-frequency impedance modulus of up to 1 GΩ cm^2 stable during 18 days in 3.5 wt% NaCl solution, a value of about five orders of magnitude higher than that of bare steel [15]. Thereafter, by varying the ethanol/H$_2$O ratio of the inorganic phase, dos Santos et al. have related the high connectivity of the silica phase (~83%) to the excellent corrosion resistance, with an almost unchanged impedance modulus of 1 GΩ cm^2 during more than 6 months immersed in saline solution and more than 3 months in saline/acid medium (Fig. 17.5) [12]. Ammar and coworkers have also studied the optimum amount of silica in acrylic—SiO$_2$ coatings deposited on mild steel. By incorporating SiO$_2$ nanoparticles into the acrylic matrix, they found an improvement of the corrosion protection for concentrations in the range of 3—8 wt%, yielding an impedance modulus of some GΩ cm^2, which remained essentially unchanged during 90 days in 3.5 wt% NaCl solution. The authors attributed the high protection efficiency to a denser physical barrier and improved adhesion of the nanocomposite coating to the steel substrate [16].

As a further step to improve the anticorrosion performance of acrylic—silica coatings, the inclusion of cathodic inhibitors such as cerium ions has been investigated due to their ability to precipitate as a protective oxide/hydroxide layer in corroded or artificially scratched regions, thus significantly increasing the durability of the coating [8,17,18]. Harb et al. have reported a significant lifetime improvement of PMMA—silica coatings modified with ceric ammonium nitrate as source of Ce(IV) ions, deposited on sanded A1010 carbon steel, with a thickness of 2 µm [8]. For intermediate Ce concentration (700 ppm), the PMMA—silica coatings have shown in potentiometric polarization curve experiments low current densities of
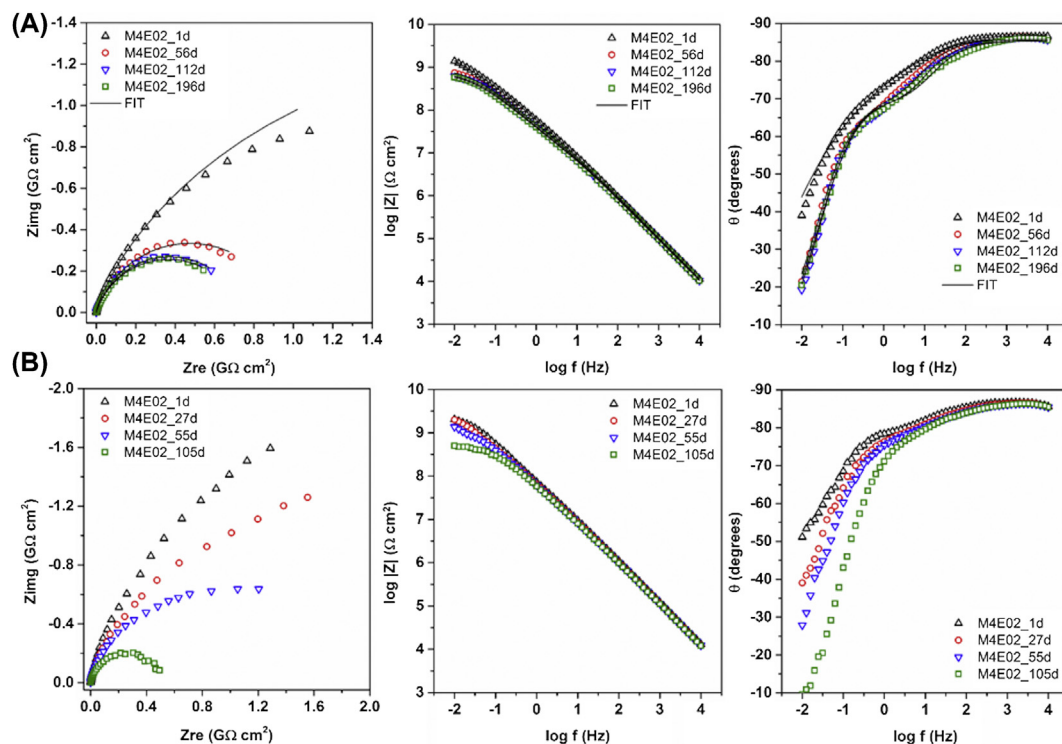
FIGURE 17.5 Nyquist and bode plots of poly(methyl methacrylate)−silica coating deposited on A1010 carbon steel immersed in (A) 3.5 wt% NaCl and (B) 0.05 mol/L NaCl + 0.05 mol/L H_2SO_4 solution [12]. *Reproduced by permission of The Royal Society of Chemistry.*

about 10^{-11} A/cm^2 at a potential of $+0.3$ V and a low-frequency impedance modulus of >0.1 GΩ cm^2 after 304 days in 3.5 wt% NaCl solution (Fig. 17.6). Moreover, the self-healing ability has been evidenced by XPS for coatings with high Ce content (>5.000 ppm) maintaining the impedance modules above 10 MΩ cm^2 during 1 year of immersion. An increase in corrosion efficiency, durability, thermal stability, hydrophobicity, and mechanical strength has also been achieved by the incorporation of lignin [19], carbon nanotubes, and graphene oxide (GO) [20], used as reinforcement agents.

Other notable results have been reported for the corrosion protection of aluminum alloys, extensively used in the aeronautic industry. The high corrosion resistance (impedance modulus >10 GΩ cm^2) and durability (>560 days) in saline solution of PMMA−silica coatings deposited on AA2024 alloy (<10 μm thickness) was related with their dense and cross-linked structure [1]. Using a copolymer system, 2-ethylhexylacrylate-co-glycidyl methacrylate, Khelifa and coworkers observed that an optimum amount of silica nanoparticles (10−30 wt%) improved the barrier properties of coated AA1050 aluminum alloy, with a low-frequency impedance modulus up to 1 GΩ cm^2, unchanged for 21 days in 0.1 M NaCl solution [13]. Additionally, they observed an increase of adhesion (ASTM D3359-D3002 peel-off method) by applying an intermediate layer of silica nanoparticles, grown by
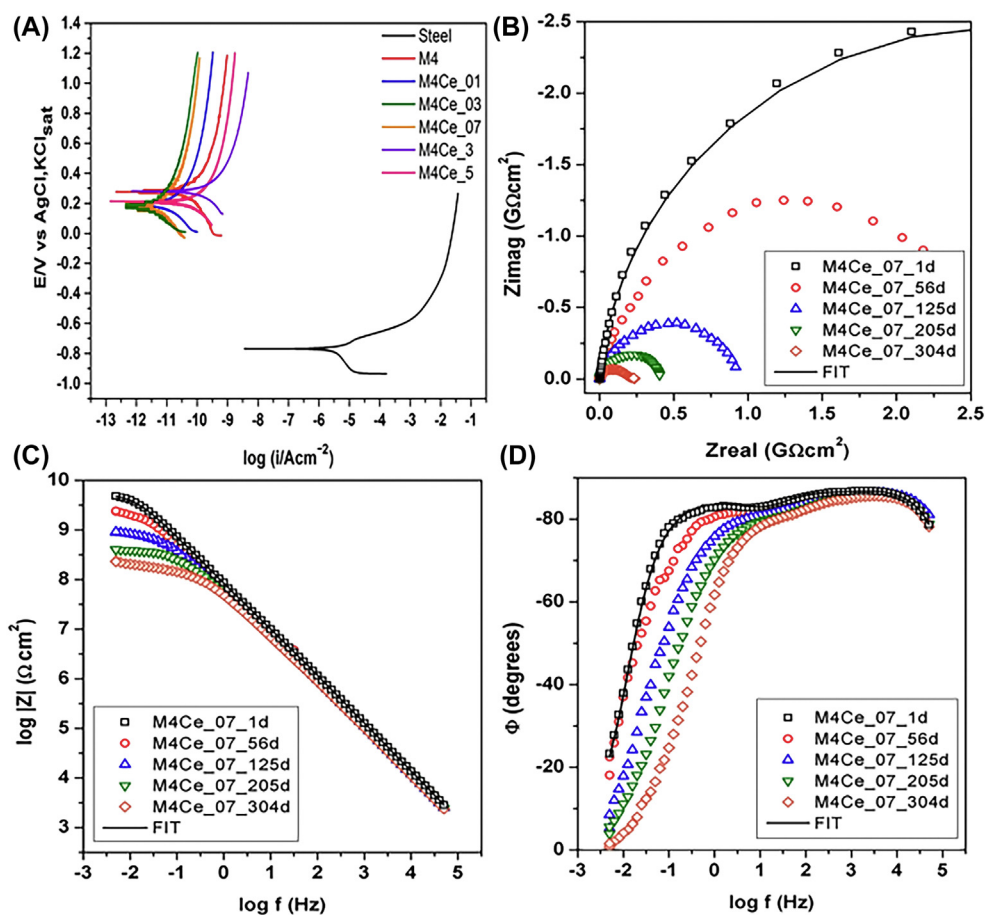
FIGURE 17.6 (A) Potentiodynamic polarization curves, (B) Nyquist plots, and (C—D) Bode plots of poly(methyl methacrylate)—silica—Ce coating deposited on carbon steel and immersed in 3.5 wt% NaCl solution [8]. *Reproduced by permission of The Royal Society of Chemistry.*

plasma-enhanced chemical vapor deposition on the aluminum surface [21]. For this system, the electrochemical results showed an unchanged anticorrosion performance during 35 days in 0.1 M NaCl solution with an impedance modulus of 1 GΩ cm^2 [21].

An overview of the recent advances in corrosion protection of high-performance acrylic nanocomposites coatings is given in Table 17.1. This data compilation is based on reported results of electrochemical analyses and compares for different coating formulations, layer thickness and substrates, best values of low-frequency impedance modulus (EIS), current density, potential and coating lifetime, parameters considered essential to evaluate the performance of anti-corrosion coatings. As can be observed in Table 17.1, an optimized formulation of the nanocomposite guarantees efficient protection of metallic surfaces, preserving their integrity in harsh environments for over a year.

TABLE 17.1 Results of electrochemical analysis obtained for best performing acrylic nanocomposite coatings applied for corrosion protection of metal surfaces: impedance modulus at low frequency, $|Z_{lf}|$, obtained by EIS; current density, I, at potential, E, extracted from potentiodynamic polarization curves; and coating lifetime in aggressive medium.

Coating	Substrate	Deposition, Thickness (μm)	$\|Z_{lf}\|$ (GΩ cm²), Lifetime (days), Solution	I (A/cm²), E (V), ref. Electrode	Ref.
PMMA–MPTS–TEOS	316L stainless steel	Dip coating ~2	~0.01 36 3.5% NaCl	10^{-9} 0.1 Ag/AgCl	[18]
Acrylic resin–SiO₂	Mild steel	Brush method 75	~10 90 3.5% NaCl	—	[16]
PMMA–MPTS–TEOS	A1010 carbon steel	Dip coating 1.5–2	~5 196 3.5% NaCl	—	[12]
PMMA–MPTS–TEOS	A1010 carbon steel	Dip coating 1.5–3	~1 18 3.5% NaCl	10^{-10} −0.3 Ag/AgCl	[15]
PMMA–MPTS–TEOS	AA2024 Al alloy	Dip coating ~3	~50 >560 3.5% NaCl	— −0.68 Ag/AgCl	[1]
GMA–EHA–GPTMS–TEOS	AA1050 Al alloy	Spin coating ~1	~1 21 0.1 M NaCl	—	[13]
PMMA–MPTS–TEOS–Ce(IV)	A1010 carbon steel	Dip coating ~2	~10 304 3.5% NaCl	10^{-11} +0.3 Ag/AgCl	[8]
PMMA–MPTS–TEOS–Ce	Mild steel	Dip coating ~26	~10 362 3.5% NaCl	10^{-12} +0.35 SCE	[17]
PMMA–MPTS–TEOS–lignin	A1020 carbon steel	Dip coating ~2	~0.5 50 3.5% NaCl	—	[19]
Acrylic resin–silanol–ZnO	Mild steel	Brush method 75	~10 30 3.5% NaCl	—	[9]
PMMA–MPTS–TEOS–CNTs or GO	A1020 carbon steel	Dip coating 3–6 μm	~3 211 3.5% NaCl	— +0.58 Ag/AgCl	[20]

CNTs, carbon nanotubes; *EHA*, 2-ethylhexyl acrylate; *EIS*, electrochemical impedance spectroscopy; *GMA*, glycidyl methacrylate; *GO*, graphene oxide; *GPTMS*, (3-glycidoxypropyl)trimethoxysilane; *MPTS*, 3-(trimethoxysilyl)propyl methacrylate; *PMMA*, poly(methyl methacrylate); *PPC*, potentiometric polarization curve; *SCE*, standard calomel electrode; *TEOS*, tetraethoxysilane.

Since these performance features can be achieved without special surface treatment and thinner coatings, than those of conventional paint systems, implies lower costs and resource savings. Further advantages are the mild conditions of preparation and use of nontoxic reagents, providing a real alternative for developing safe and economic materials to replace the toxic hexavalent chromium conversion coatings still used at a large scale to protect aluminum alloys.

Although organic—inorganic nanocomposites have been manufactured on an industrial scale since the 1940s [11], acrylic nanocomposites show a very modest presence in the primer and coatings' market. Therefore, the main challenges are to advance the production and application of hybrid nanocomposites on an industrial scale and to improve the lifetime prediction in corrosive environments using theoretical simulations that allow determining the processes involved by tracking the evolution of physical quantities during electrolyte permeation, as reported recently using the Young model [21a].

3. Epoxy-based nanocomposite

Epoxy resins are irreversibly hardened (cured) by cross-linking the individual polymer chains, forming rigid and thermally stable thermosetting epoxy polymers. These polymers are obtained by the reaction between the reactive groups of the hardener (amines, epoxies, dicyandiamide, isocyanates, among others) and epoxy functional group of organic resins. Epoxy resins, such as poly(bisphenol A-co-epichlorohydrin) glycidyl end-capped, epoxyphenol novolak, and butyl glycidyl ether, are obtained by the reaction between epichlorohydrin and (1) bisphenols (bisphenol A, bisphenol F, bisphenol AF, bisphenol S, etc.), (2) novolaks, which are produced by reacting phenol with methanal (formaldehyde), or (3) aliphatic alcohols, polyols, or carboxylic acids, although the latter form of epoxy resin is more used as flexibilizers or diluent for the others types of resins (Fig. 17.7).

The epoxy functional groups, also known as oxirane, impart the reactivity to this family of materials. This is due to the high bonding stress of the epoxy ring, forming a triangular carbon—oxygen—carbon (—COC—) bond arrangement, which facilitates its opening by a wide range of reactants (curing agents). The formation of the three-dimensional epoxy network can occur at room temperature or at elevated temperatures depending on the nature of the curing agent. The mostly used curing agents are nitrogen-containing molecules having functionality equal or higher than three ($f \geq 3$), for example, polyamines and their derivatives. The functionality is the number of available bonding sites, such as $f = 4$ for diamino diphenyl methane, $f = 6$ for triethylenetetramine, and $f = 5$ for diethylenetriamine (Fig. 17.8A) [22]. The curing reactions proceed by SN_2 nucleophilic attack of the nitrogen electrons from the curing agent to the least substituted carbon of the oxirane ring, resulting in its opening and formation of an OH group (Fig. 17.8B). The formed secondary amine nitrogen, even though less reactive, attacks another epoxy ring, resulting in 3D cross-linking that significantly improves the thermal, mechanical, and chemical stability of the polymer [22]. Other important properties include high chemical resistance, especially in alkaline environments, good adhesion to metallic substrates, curing ability over a wide range of temperatures, and high corrosion resistance as a coating material [23].
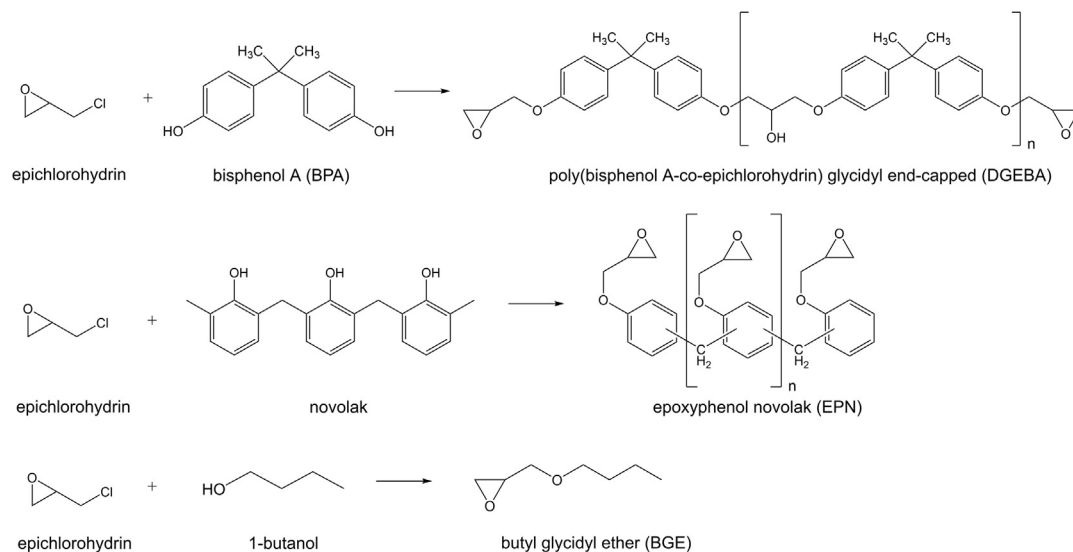
FIGURE 17.7   Structural representation of epoxy resins obtained from the reaction between epichlorohydrin with bisphenol, novolak, and aliphatic epoxy resin.
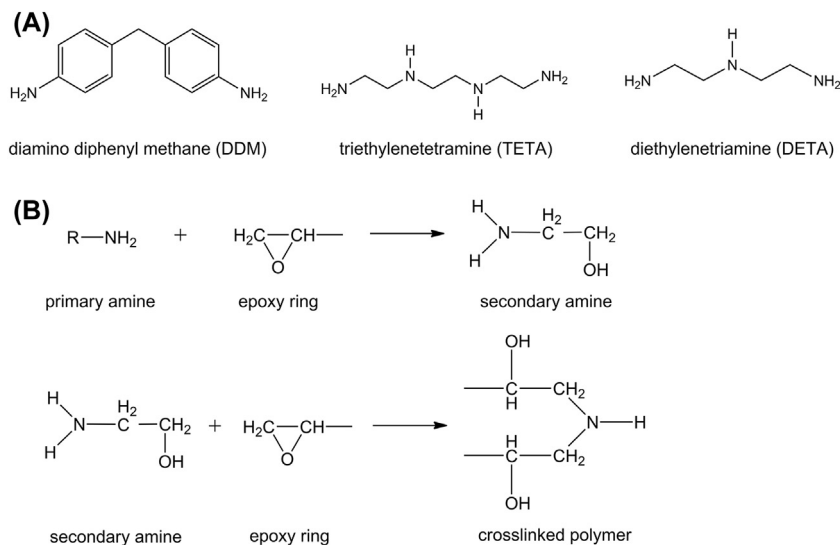
FIGURE 17.8   (A) Structural representation of commonly used curing agents for epoxy resins, and (B) formation of a thermosetting cross-linked polymer by the reaction of curing agents, containing amine functional groups, with the epoxy ring of the resin.

Further improvements of epoxies can be achieved by the introduction of organic and inorganic nanofillers (inorganic compounds, nanocontainers with corrosion inhibitors, among others), interacting either covalently or by van der Waals forces with the organic matrix. In

the case of covalent conjugation of epoxy with inorganic compounds, typically oxide nanoparticles, a coupling agent is used, forming an organic—inorganic interphase. Here the nitrogen nucleophilic attack of the hardener occurs on both the epoxy group of the resin and the epoxy group of the coupling molecule, such as (3-glycidyloxypropyl)trimethoxysilane (GPTMS) (Fig. 17.4). This molecule is frequently used as coupling agent in the synthesis of organic—inorganic nanocomposites due to its ability to conjugate covalently the epoxy phase with silica nanoparticles, although several other molecules can also be used for this purpose, such as 3-(2-aminoethylamino)propyl dimethoxymethylsilane (AEAPS) and (3-aminopropyl)triethoxysilane (APTES) (Fig. 17.4), both forming covalent bond through their amino functional groups [14]. The properties of the epoxy-based nanocomposites depend on the chemical structure of the monomer, type, and amount of nanofiller and the nature and quantity of the curing and coupling agent, both defining the overall connectivity of the final structure [22,23]. Consequently, the fine-tuning of these parameters allows tailoring their final properties for a wide variety of applications.

For application in protective coatings, epoxy nanocomposites profit from their cross-linked polymeric structure in terms of higher thermal, mechanical, and chemical stability and particularly improved barrier property. The electrochemical performance reported for different types of anticorrosion epoxy nanocomposite coatings is summarized in Table 17.2.

Among the best performing coatings reported so far are epoxies modified with polyaniline (PANI), applied to protect the surface of mild steel. A low-frequency impedance modulus of $400\,G\Omega\,cm^2$ and life span of 60 days in 12 wt% NaCl solution was achieved by dispersing PANI nanorods in commercial epoxy resin and curing using commercial cardanol-based polyamide agent (Table 17.2) [24]. A different type of epoxy coating, prepared from commercial epoxy resin, based on bisphenol A, was doped with sulfonated PANI nanofibers and deposited on mild steel. The coatings presented a low-frequency impedance modulus between 10 and $100\,G\Omega\,cm^2$ and durability of 120 days immersed in 3.5 wt% NaCl solution [25].

Another interesting class of nanocomposites for corrosion protection of steel are epoxy nanocomposites modified with graphene oxide (GO). The coatings were prepared using an epoxy resin derived from bisphenol A (EPON Resin 828), cross-linked by cycloaliphatic amine—based curing agent (Epikure F205) and modified with an additive based on GO, PANI nanofibers, and CeO_2 nanoparticles. The filler addition resulted in a significant improvement of the corrosion protection reaching a low-frequency impedance modulus of $1.6\,G\Omega\,cm^2$, maintained stable for 70 days in 3.5 wt% NaCl solution (Table 17.2) [26]. Another study reports on the modification of a commercial epoxy resin with GO encapsulated by ZrO_2 nanoparticles. According to the authors, the ZrO_2-GO nanofiller was capable of blocking local microgalvanic corrosion, in addition to filling defects in the coating, yielding an impedance modulus of $82\,G\Omega\,cm^2$ after 60 days in contact with 3.5 wt% saline solution [27].

Excellent anticorrosion efficiency has been achieved also for organic—inorganic hybrids, combining the polymer curing reaction with the sol—gel process used to prepare the inorganic phase. Epoxy—silica coatings prepared using poly(bisphenol A-co-epichlorohydrin) glycidyl end-capped (DGEBA), diethylenetriamine (DETA) as hardener, GPTMS as coupling agent, and tetraethoxysilane (TEOS) as silica source were applied on carbon steel. The coating exhibited for the best formulation (molar ratio DGEBA:DETA:GPTMS:TEOS = 8:0.3:8:8) an impedance modulus of $\sim 1\,G\Omega\,cm^2$, after immersion in 3.5 wt% saline solution, and durability of 42 days [28]. To study the influence of the curing agent on the anticorrosion efficiency

TABLE 17.2   Results of electrochemical analysis obtained for best performing epoxy nanocomposite coatings applied for corrosion protection of metal surfaces: impedance modulus at low frequency, $|Z_{lf}|$, obtained by electrochemical impedance spectroscopy, and current density, I, at potential, E, extracted from polarization curves.

Coating	Substrate	Deposition, Thickness (μm)	$\|Z_{lf}\|$ (GΩ cm^2), Lifetime (days), Solution	I (A/cm^2) E (V), Electrode	Ref.
Epoxy−GPTMS−TEOS	Carbon steel	Dip coating ~8−9	~10 30 3.5 wt% NaCl	−	[This work]
Epoxy−APTES	Carbon steel	Spray 125	~100 21 0.1 M Na$_2$SO$_4$	−	[40]
Epoxy−polysiloxane (APTES/ APTMS/GPTMS/TMSPh)	Mg alloyAZ31	Dip coating 12	~5 28 0.05 M NaCl	−	[30]
Epoxy−APTES	Mg alloy AZ31	Dip coating ~14	10 31 3.5 wt% NaCl	−	[29]
Epoxy−zinc phosphate−iron oxide	Cold rolled low carbon steel	Airless spray 55−140	~450/60 220/405 3 wt% NaCl	−	[41]
Epoxy−PDMS−ZnO	Mild steel	Brush method 70−80	100 30 3 wt% NaCl	−	[33]
Epoxy−GO−Closite20A	Steel	Film applicator 75−90	10 ~56 3.5 wt% NaCl	−	[42]
Epoxy−PANI	Mild steel	Film applicator 20	10−100 120 3.5 wt% NaCl	10^{-7} −0.61 SCE	[25]
Epoxy−PANI	Mild steel	Brush method 120	400 80 12 wt% NaCl	−	[24]
Epoxy−GO−P2BA	Q235 carbon steel	Film applicator 20	10 80 3.5 wt% NaCl	10^{-11} −0.34 SCE	[43]
Epoxy−PDMS−SiO$_2$	Mild steel	Brush method ~71−74	100 30 3 wt% NaCl	−	[34]
Epoxy−APTES-3 −methylsalicylate	Commercial pure Mg	Dip coating ~13−17	90 35 3.5 wt% NaCl	−	[32]

TABLE 17.2   Results of electrochemical analysis obtained for best performing epoxy nanocomposite coatings applied for corrosion protection of metal surfaces: impedance modulus at low frequency, $|Z_{lf}|$, obtained by electrochemical impedance spectroscopy, and current density, I, at potential, E, extracted from polarization curves.—cont'd

Coating	Substrate	Deposition, Thickness (µm)	$|Z_{lf}|$ (GΩ cm²), Lifetime (days), Solution	I (A/cm²) E (V), Electrode	Ref.
Epoxy–reduced GO	Q235 carbon steel	Film applicator 120	~20 60 3.5 wt% NaCl	–	[44]
Epoxy–APTES–ZrO₂_GO	Q235 carbon steel	Film applicator 140	~80 60 3.5 wt% NaCl	–	[27]
Epoxy–PANI–CeO₂_GO	Mild steel	– 75	~1.6 70 3.5 wt% NaCl	–	[26]
Epoxy–dye-clay nano pigment	Mild steel	Film applicator 30	~20 35 3.5 wt% NaCl	–	[31]
Epoxy–GPTMS–TEOS	Stainless steel	Dip coating ~2–7	~1 42 3.5 wt% NaCl	–	[28]
Epoxy–APTES–CeO₂	Mg alloy AZ31	Dip coating ~10	~10 29 0.05 M NaCl	–	[35]
Epoxy–GO–PANI–Zn	Mild steel	Film applicator 65–115	~1 ~77 3.5 wt% NaCl	–	[45]
Epoxy–MoS₂_PDA	Carbon steel	– ~50	10 20 3.5 wt% NaCl	10^{-10} −0.08 Ag/AgCl	[36]
Epoxy–SiO₂	Mild steel	Spray 41–43	~100 30 3.5 wt% NaCl	–	[37]
Epoxy–SiO₂–MBI–PEG	Carbon steel	Film applicator 30	~1 42 3.5 wt% NaCl	10^{-10} −0.02 Ag/AgCl	[38]
Epoxy–APTES–tetrathiol	Al alloy AA2024-T3	Single blade 150	~1 350 0.5 M NaCl	–	[39]

APTES, aminopropyltriethoxysilane; *APTMS*, aminopropyltrimethoxysilane; *GO*, graphene oxide; *GTPMS*, (3-glycidoxypropyl)trimethoxysilane; *MBI*, 2-mercaptobenzimidazol; *P2BA*, poly(2-butylaniline); *PANI*, polyaniline; *PDA*, polydopamine; *PDMS*, polydimethylsiloxane; *PEG*, poly(ethylene glycol); *TEOS*, tetraethoxysilane; *TMSPh*, tris(trimethylsilyl)phosphate.

of these coatings on carbon steel, the proportion between the hardener and bisphenol was evaluated for samples with DETA to DGEBA molar ratios of 2.4, 3.2, and 4.8, referred to as D2.4, D3.2, and D4.8. Bode impedance modulus plots recorded for different immersion periods in 3.5 wt% NaCl solution (Fig. 17.9) show the best result for the highest molar fraction (D4.8). This coating, with a thickness of 9 μm, showed a low-frequency impedance modulus of 10 GΩ cm^2 after 1 day and ∼1 GΩ cm^2 after 30 days in contact with 3.5 wt% NaCl solution, a value still four orders of magnitude higher than that of bare carbon steel.

For coatings based on poly(bisphenol A-co-epichlorohydrin) glycidyl end-capped and APTES, deposited on magnesium alloy AZ31, the low-frequency impedance modulus reached values up to 10 GΩ cm^2 in 3.5 wt% NaCl solution and lifetime of 31 days (Table 17.2) [29]. Another class of high-performance coatings was prepared by Brusciotti and coauthors. They showed that epoxy−silica nanocomposites prepared by the variation of organosilane species (APTES, APTMS: aminopropyltrimethoxysilane, GTPMS: (3-glycidoxypropyl)trimethoxysilane, and TMSPh: tris(trimethylsilyl)phosphate) yield coatings with impedance modulus up to 5 GΩ cm^2 in 0.05 M NaCl solution, stable for 29 days [30].

Table 17.2 shows the large variety of modifying agents used to prepare epoxy coatings yielding high corrosion protection efficiency for different metallic surfaces, such as pigments [31]; nanocontainers loaded with corrosion inhibitor [32]; and inorganic nanoparticles (CeO$_2$, SiO$_2$, ZnO, MoS$_2$) [26,33−38]. Remarkable results were reported by Zadeh et al. for self-healing epoxy coatings containing tetrathiol-sufonated groups [39]. The coating with a molar ratio between pentaerythritol tetrakis (3-mercaptopropionate) and bis[3-(triethoxysilyl) propyl]tetrasulfide equal to 3:1 exhibited a hydrophobic surface, high adhesion strength to the aluminum AA2024-T3 alloy, and effective corrosion protection in 0.5 M NaCl solution with low-frequency impedance modulus of 3 GΩ cm^2 and durability of 350 days. Moreover, after artificial damaging and subsequent heat treatment, the coatings showed the healing effect ability, restoring their barrier property [39].
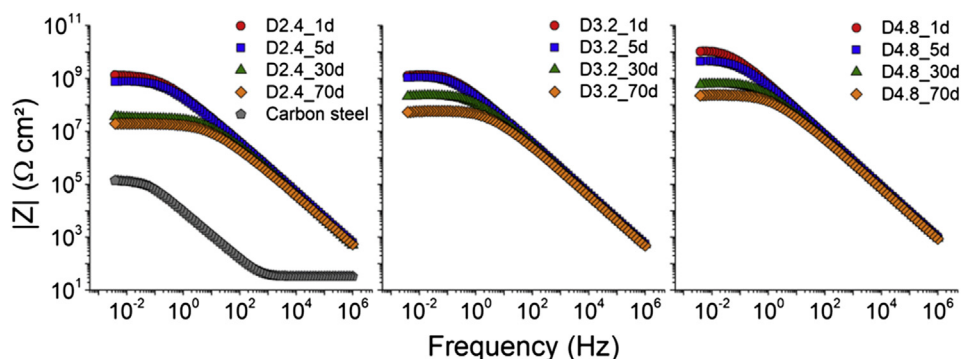

FIGURE 17.9 Bode plots of the impedance modulus versus frequency for different immersion times in 3.5 wt% NaCl solution obtained for epoxy−silica coating with different hardener (DETA) to bisphenol (DGEBA) ratios, deposited on carbon steel. DETA, diethylenetriamine; DGEBA, poly(bisphenol A-co-epichlorohydrin) glycidyl end-capped.

The growing concern about the depletion of fossil reserves and the emission of greenhouse gases has contributed to the development of polymers derived from renewable sources. In this context, epoxy resins derived from biologically based chemicals are of special interest for the development of thermosets with promising properties. As a starting material for the synthesis of the biothermosets, a wide variety of rigid ring structures or more reactive groups can be found, such as rosin acid, diphenolic acid, tannin acid, itaconic acid, glucose, eugenol, furan, and isosorbide [46].

4. Polyurethane-based nanocomposites

Another interesting class of polymeric nanocomposite coatings is based on polyurethane (PU), which is a polymer most commonly formed by reacting a di- or tripolyisocyanate, e.g., toluene diisocyanate, methylene diphenyl diisocyanate, and 1,6-hexamethylene diisocyanate, with a polyol, e.g., dipropylene glycol, glycerin, and sorbitol, yielding organic units linked by carbamate (urethane) groups (Fig. 17.10). In recent years, the preparation of PUs from green sources received increasing attention since the PU industry is dependent on fossil-based polyols. Aiming to confer new functionalities, as biodegradability and biocompatibility, variations of protective coatings include mainly vegetable oil–based materials [47–50] and also carbohydrates [51].

Among the most common forms of the versatile polyurethanes are soft and rigid foams, elastomers, adhesives, plastic films, and, in particular, anticorrosive coatings, which have shown promising results. The functionality of polyurethane can be tailored according to
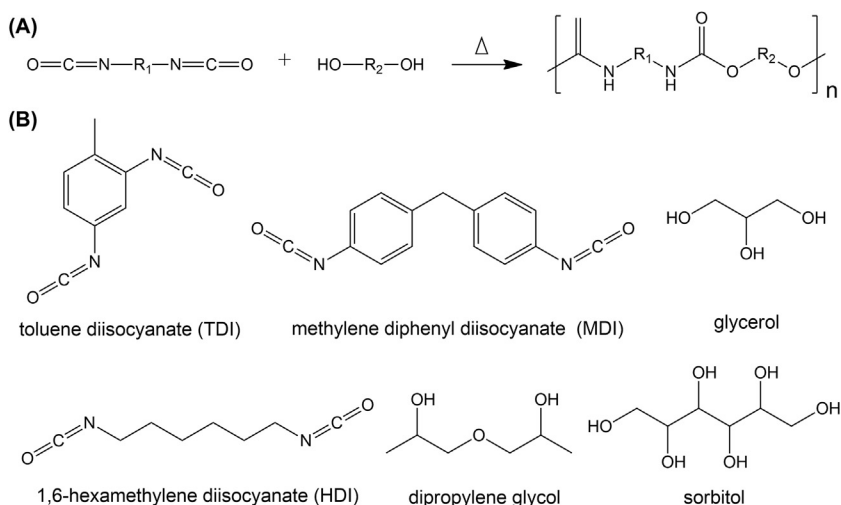

FIGURE 17.10   (A) Structural representation of polyurethane preparation through reaction of isocyanate groups (R–N=C=O) with hydroxyls from polyol, and (B) structure of most common polyurethane precursors. *(A) Adapted from K. van Rijswijk, H.E.N. Bersee, Reactive processing of textile fiber-reinforced thermoplastic composites – an overview, Compos. Part A Appl. Sci. Manuf. 38 (2007) 666–681.*

the application: to obtain thermoplastic polymers, the linear chains must be designed with two isocyanate and polyol functionalities, whereas for thermosetting polymers, more than two functions of one of the parts (or both) are required to provide cross-linking. In practice, most polyurethanes are thermosetting polymers that exhibit high mechanical strength and thermal stability.

For the synthesis of most polyurethanes, the choice of the catalyst is fundamental to obtain the desired material properties. The use of catalysts reduces the reaction time and allows complete curing of the material at low temperatures. Currently, organometallic tertiary amines and tin compounds (1,4-diazabicyclo[2.2.2]octane and dibutyltin dilaurate, respectively) are some of the most commonly used catalysts. Especially in the reaction between alcohols and isocyanates, they not only increase the speed of the reaction but also influence the selectivity of the final product [52].

Polyurethane paints are often applied as topcoats on a epoxy primer layer due to their abrasion and chemical resistance, making them suitable for offshore environment with high UV exposure and aggressive saline media. An almost unchanged performance with an impedance modulus of 100 MΩ cm^2 during 100 days of exposure to 3.5% NaCl was reported for polyurethane—urea hybrid coatings [53], confirming their elevated barrier properties. In other recent studies, polyurethane-based nanocomposite coatings with a low corrosion rate ($\sim 10^{-4}$ mm/year) [54] and high corrosion resistance (100 GΩ cm^2 low-frequency impedance modulus) [55—58] were reported for different metallic substrates. For instance, Maya-Visuet et al. observed elevated long-term stability of 263 days in saline/acid media (3.5% NaCl solution at pH 5) for 50—75 μm thick polyurethane composite coatings containing TiO$_2$ as ceramic nanofiller (Fig. 17.11) [55]. Del Algel-López et al. reported on

FIGURE 17.11   Bode plots for different immersion times recorded for polyurethane composite coatings loaded with 10 wt% TiO$_2$ immersed in an acidic environment (3.5% NaCl solution at pH 5) [55]. *Reproduced with permission of Elsevier.*
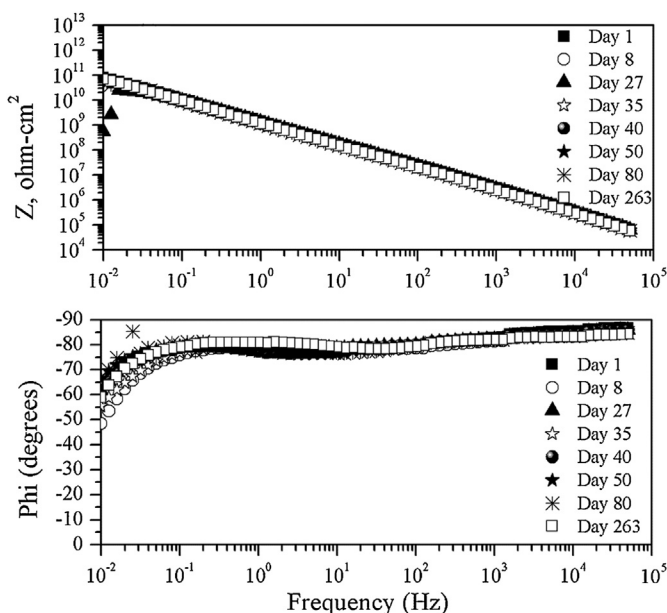
polyurethane coatings (40–55 μm) loaded with $ZrO_2:SiO_2$ (25:75) nanoparticles, which resisted for 226 days in saline environment (3% NaCl) [56].

A variety of fillers have been used to strengthen the PU matrix in terms of hardness, stiffness, thermal resistance, and corrosion inhibition, such as SiO_2 [54,56,59], $ZrO_2:SiO_2$ [56], TiO_2 [55], CeO_2 [60], Ce(IV)/carbon nanotubes [61], GO [57,62], bisphenol A [63], urea [53], ZnO [64], and Cloisite 30B montmorillonite [65]. To improve the connectivity between the polymeric phase and the inorganic additives, some authors used cross-linking agents [52,55], mainly in the form of organosilane molecules (Fig. 17.4). The potential of polyurethane-based nanocomposites in the field of protective coatings is reflected by the increasing number of recent studies, with the best results summarized in Table 17.3.

Besides passive corrosion protection, polyurethane coatings can present self-healing property, thanks to the shape-recovery ability of polycaprolactone and isobornylacrylate additives. They provide mobility to the polymer chain above 60 °C, allowing to heal defective zones by heating. Lutz et al. incorporated layered double hydroxides loaded with 2-mercaptobenzothiazole to achieve intrinsic and extrinsic (heating) inhibition of polyurethane. Besides providing an impedance modulus of about 10 GΩ cm^2 in 0.05 M NaCl, the coating showed the ability to seal macrodefects and restore the corrosion protection [70]. Furthermore, polyurethane can be modified with bioactive compounds, such as hydroxyapatite, and act as biocompatible and anticorrosive coating, delaying the corrosive attack of AZ31 Mg alloy for 101 days in Hank's solution [69].

The current demand for green, versatile, and multifunctional materials urges for the development of thin ($\sim$ μm), adherent, and environmentally friendly coatings with active protection, capable to substitute conventional systems based on chromates and paints. Hence, the big variety of formulations of polymeric nanocomposites based on polyurethanes allows to tailor their final properties such as low permeability, super hydrophilicity, self-healing, self-cleaning, and ice repellent properties. All these features are of great interest for applications in protective coating, portable electronics, car industry, and aircraft manufacture. However, the biggest challenge is to improve the long-term stability of the coatings in aggressive environments.

5. Other classes of polymeric nanocomposites

5.1 Fluoropolymers

Fluoropolymers or fluoroplastics comprise a class of polymers that contain in their chemical structure mainly carbon and fluorine. The physical and chemical properties of fluorine give the compounds exceptional resistance to chemicals, such as organic solvents, acids, and inorganic bases, which are of great interest for the development of high-performance anticorrosive coatings [71]. Moreover, the presence of a continuous and uniform arrangement of fluorine atoms around carbon atoms provides other important features, such as high thermal stability, low refractive index, low electrical and friction resistance, low surface energy, and nonstick property. In addition, the high electronegativity of fluorine yields a highly hydrophobic surfaces with repulsive effect against corrosive electrolytes [71,72].

TABLE 17.3   Results of electrochemical analysis obtained for best performing polyurethane nanocomposite coatings applied for corrosion protection of metal surfaces: low-frequency impedance modulus $|Z_{lf}|$, obtained by electrochemical impedance spectroscopy; current density, I, at potential, E, extracted from polarization curves.

Coating	Substrate	Deposition, Thickness (μm)	$\|Z_{lf}\|$ (GΩ cm^2), Lifetime (days), Solution	I (A/cm^2) E (V), Electrode	Ref.
Polyurethane−ZrO$_2$−SiO$_2$	Carbon steel	Spray 40−55	∼100 226 3.5% NaCl	−	[56]
Polyurethane−epoxy−acrylate−GO	Carbon steel	Brush method ∼70	∼100 21 5% NaCl	10^{-11} −0.1 Ag/AgCl	[57]
Polyurethane−PANI	Mild steel	Brush method ∼60	∼10 58 3.5% NaCl	−	[66]
Polyurethane−graphene	Phosphated steel	Film casting knife ∼100	∼1 28 3.5% NaCl	10^{-11} −0.02 SCE	[67]
Polyurethane−CNTs	Phosphated steel	Wire lab rod ∼50	∼0.1 28 3.5% NaCl	10^{-10} 0.1 SCE	[68]
Polyurethane−urea	Carbon steel	−	∼0.1 100 3.5% NaCl	−	[53]
Polyurethane−polydiphenylamine−V$_2$O$_5$	Carbon steel	Brush method ∼90	∼100 30 5% NaCl	10^{-11} −0.04 −	[58]
Polyurethane−MMT	Carbon steel	Film applicator ∼40	∼10 225 3.5% NaCl	−	[65]
Polyetherimide−HA	Mg alloy AZ31	Dip coating ∼4	∼1 101 Hank's solution	−	[69]
Polyurethane−APTES−TEOS−TiO$_2$	AA3003 H14	Drawdown bar 75	∼263 3.5% NaCl + 0.1 M HCl	−	[55]

APTES, aminopropyltriethoxysilane; *CNTs*, carbon nanotubes; *GO*, graphene oxide; *HA*, hydroxyapatite; *MMT*, montmorillonite; *PANI*, polyaniline; *SCE*, standard calomel electrode; *TEOS*, tetraethoxysilane.

Various types of fluoropolymers, such as poly(vinyl fluoride), poly(tetrafluoroethylene) (PTFE), and poly(vinylidene fluoride), have found wide range of applications in various fields including coating (Fig. 17.12). Among them, the PTFE, known as Teflon, is obtained by polymerization of tetrafluoroethylene in the form of linear chains and has many applications in domestic utensils and industrial equipment.
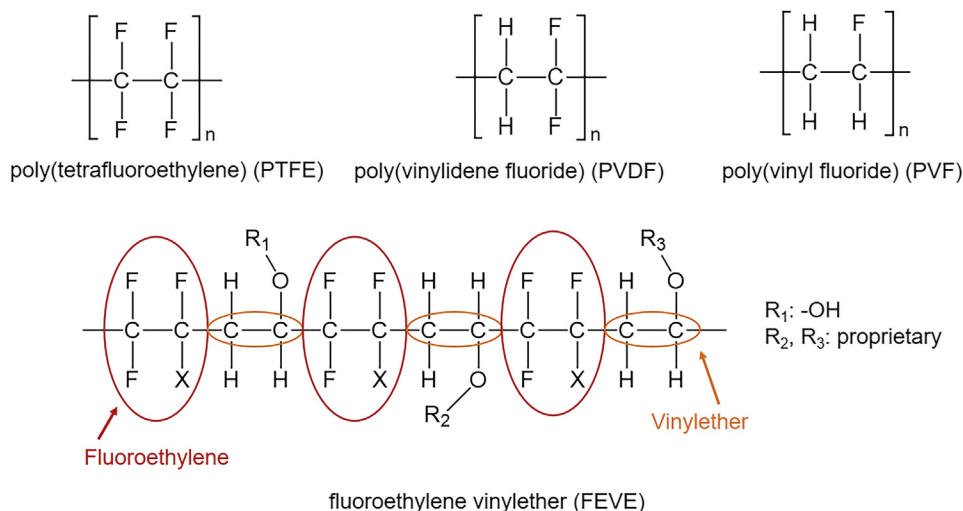
FIGURE 17.12   Structural representation of some common fluoropolymers.

Several fluoropolymers [73–78] and their nanocomposites have been studied as protective coatings; however, only few of them exhibited high anticorrosive performance in aggressive environments in terms of low-frequency impedance modulus higher than 0.1 GΩ cm^2 and durability of more than 30 days. The most commonly used polymer for low-temperature preparation of fluoropolymer-based nanocomposites is the fluoroethylene vinylether (FEVE), consisting of CF$_2$-CFX blocks and functional groups attached to the polymer backbone (Fig. 17.12). As an example of high-performance nanocomposite coatings, the commercial FEVE copolymer (Lumiflon LF-200) has been prepared with different isocyanate-based curing agents and modified with polyhedral oligomeric silsesquioxane [79]. The coating deposited on bronze discs with a thickness of ∼5 µm exhibited an impedance modulus of about 1 GΩ cm^2 after 3 h of immersion in 0.5 M NaCl solution and a decrease of one order of magnitude after 6 days, remaining stable for a period of 140 days.

Although the anticorrosive efficiency of most fluoropolymers has not reached outstanding results, such as acrylates, epoxies, and polyurethanes, this class of material is very promising for multifunctional coatings and should be further studied to achieve high anticorrosive performance. Specially, organic—inorganic nanocomposites containingcovalent coupling molecules result in an enhanced anti-corrosion performance.

5.2 Conducting polymers

In 1985, DeBerry reported that a PANI coating deposited on ferritic stainless steel provided anodic protection, significantly reducing the corrosion rate in an acid environment [80]. Since then, conducting polymer nanocomposites have gained increasing attention as anticorrosive coatings, especially those based on polyaniline (PANI). PANI is a conducting polymer formed by the polymerization of aniline, an organic compound consisting of a phenyl group attached to an amino group. PANI is generally obtained by chemical oxidative

polymerization or electrochemical polymerization [81]. The preparation of PANI requires (1) an acidic medium, where aniline exists as an anilinium cation, and (2) an oxidative environment, which can be supplied via the presence of larger amounts of oxidizing agents (such as ammonium peroxydisulfate) or by the application of potential in an electrochemical cell containing acidic aniline solution [81,82]. The resulting protonated PANI (e.g., PANI hydrochloride), called emeraldine salt can be converted into its deprotonated form in alkaline medium, obtaining the so-called emeraldine base (denoted PANI-E or PANI-EB) (Fig. 17.13A). Through reduction and oxidation reactions, emeraldine base can be transformed into leucoemeraldine (denoted as PANI-L) referred to as PANI's fully reduced form, or pernigraniline (denoted as PANI-P), referred to as PANI's fully oxidized form (Fig. 17.13A) [81]. The average oxidation state is given by the doping degree: for the fully reduced form (leucoemeraldine), the doping degree, x, is equal to zero; for the fully oxidized form (pernigraniline), it is one; and for intermediated oxidation states, it is $0 < x < 1$.

The emeraldine salt presents conductivity similar to a doped semiconductor, of about 100 S/cm, but when converted into emeraldine base, leucoemeraldine, or pernigraniline, it behaves as electrically insulating material [82]. Conducting polymeric coating can protect metals against corrosion by several mechanisms, including barrier protection, controlled inhibitor release, anodic protection, and formation of an insoluble counteranion salt [83,84]. Salem and Grgur have shown that corrosion protection is dependent on the protonation level of the PANI [85]. The authors have prepared PANI doped with sulfamic acid (0.28 of doping degree), succinic acid (0.18 of doping degree), citric acid (0.15 of doping degree), and acetic acid (0.13 of doping degree), incorporated 5 wt% into alkyd-based commercial paint, and applied the solution on mild steel using a scalpel blade—based method. The polarization resistances were determined using linear polarization method, in 3 wt% NaCl solution. The initial oxidation state of the PANI was determinant for the values of polarization resistance,
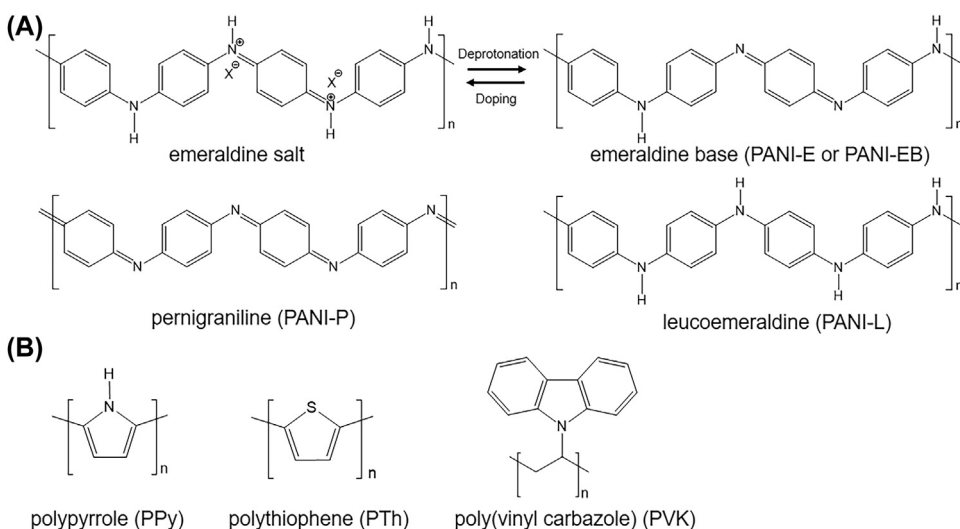

FIGURE 17.13   Molecular structure of (A) polyaniline (PANI) and (B) other conductive polymers.

which decreased in the following sequence: Rp(sulfamic) > Rp(succinic) > Rp(citric) > Rp(acetic) ∼ Rp(base coating). This result is in agreement with visual inspection of the coatings, showing that the corrosion products are more abundant for higher oxidization state PANI filler (Fig. 17.14).

Other types of conductive polymers used as protective coating include polypyrrole [86,87], polythiophene [88], and poly(vinyl carbazole) [86] (Fig. 17.13B). In general, no major differences of impedance modulus and corrosion potential have been detected between pure conductive polymeric coatings and bare alloys, indicating poor corrosion protection [86,89−91]. Even when modified with fillers, such as montmorillonite [92−94], TiO$_2$ [95,96], SiO$_2$ [86,97], Ag [95], Zn [95], graphene [98], GO [99], and carbon nanotubes [100,101], only a modest increase of the corrosion resistance has been achieved. To the best of our knowledge, no conducting polymer-based coating has achieved an impedance modulus higher than 0.1 GΩ cm^2 and lifetime longer than 30 days.

An alternative approach that has yielded good results in terms of anticorrosive efficiency is the use of conducting polymers as fillers in other polymeric matrices. Zhang and coworkers have incorporated 10 wt% of emeraldine base and salt (hydrofluoric acid−doped and camphorsulfonic acid−doped PANI) into an epoxy matrix [83]. EIS results obtained in 3.5 wt% NaCl solution showed for camphorsulfonic acid−doped PANI coatings on mild steel a high anticorrosive performance, with low-frequency impedance modulus of 51 GΩ cm^2, which decreased by only two orders of magnitude after 175 days. Structural and electrochemical analyses indicate that the addition of PANI, especially in the form of salt, leads to improved barrier property against electrolytes and after failure to the formation of a compact layer of corrosion product due to redox reaction of PANI, thus offering additional protection for the steel surface. Moreover, the coating modified by camphorsulfonic acid−doped PANI contains sulfonate ligand anions that are capable of complexing Fe, thus resulting in an inhibiting mechanism based on insoluble counteranion salt. The authors of another work reporting on high-anticorrosion efficiency PANI-modified coatings used polyaniline doped with dodecylbenzenesulfonic acid (PANI−DBSA) in epoxy resin and applied the paint by spray deposition onto steel plates (SAE 1020) [102]. The addition of 0.1 and 0.5 wt% of PANI−DBSA resulted in an increase of the coating impedance from 80 GΩ cm^2 (pure epoxy coating) to 160 and 197 GΩ cm^2, respectively. Both epoxy PANI−DBSA-modified coatings presented good durability, with only one order of magnitude decrease of the impedance modulus, after 30 days of immersion in 3.5 wt% NaCl solution [102].
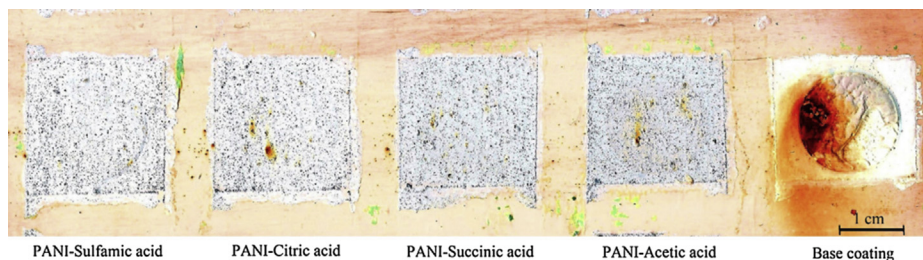

FIGURE 17.14 Coated steel substrates with alkyd paint containing polyaniline (PANI) in different oxidation states, after 238 h of immersion in 3% NaCl [85]. *Reproduced with permission of Elsevier.*

PANI has also been used combined with polyacrylates in the form of core—shell structure to protect carbon steel. The material was composed of poly(methyl methacrylate), butyl acrylate, and acrylic acid, as "core" (P(MMA/BA/AA)), and PANI—DBSA, as "shell.". The spherical P(MMA/BA/AA) nanoparticles with and without PANI-DBSA were applied as 80 μm thick coatings on phosphatized carbon steel (AISI 1005) and tested in 3.5 wt% NaCl solution. The presence of a low concentration of PANI—DBSA (3 wt%) in the acrylic polymer resulted in increased conductivity (2.7×10^{-5} S/cm, compared with 3.2×10^{-8} S/cm for pure polymer) and an improved passivation effect of the steel surface. Although the low-frequency impedance modulus was similar for both samples (~ 100 MΩ cm^2), the corrosion protection of PANI—DBSA containing coating remained effective during 18 days in saline solution [103]. Another notable result has been reported by Su et al. combining graphene, PANI (pernigraniline), and PVB for the corrosion protection of copper [104]. The nanocomposite coating with a thickness of 46 μm exhibited an impedance modulus of almost 10 GΩ cm^2 after 7 days of immersion in 0.03 M NaCl aqueous solution. The efficient corrosion protection was attributed to the well-dispersed fillers in the PVB matrix, which reduced the porosity and decreased the diffusion pathways for corrosive species.

5.3 Poly(lactic acid), polyhydroxybutyrate, polyethylene terephthalate, polybutyrate, polyvinyl chloride, polystyrene, and polyetherimide polymers

Polyester is another class of polymers that has been recently applied as anticorrosive coating on different metallic surfaces. This category of polymers contains an ester functional group in the main chain and includes naturally occurring polymers, such as poly(lactic acid) and polyhydroxybutyrate, as well as synthetics such as polyethylene terephthalate (PET) and polybutyrate (Fig. 17.15A). PET is the most common polymer resin of the polyester family, and therefore, it is usually used as a synonym of polyester.

In general, polyester-based coatings present weak resistance against electrolyte permeation; however, in the form of nanocomposites, they show significantly improved barrier property by reducing the presence of voids and percolation pathways. Some examples of modifier agents used to prepare polyester nanocomposite coatings for corrosion protection of metallic alloys include organosilane [105,106], GO [107], clay [108], zinc ferrite [109], and ZnO [110]. Mahvidi et al. prepared coatings on mild steel based on a mixture of polyester and formaldehyde resin (also called melamine), which was loaded with 0.5 wt% zinc ferrite nanoparticles [109]. While the pure polymeric coating presented a low-frequency impedance modulus of 100 MΩ cm^2, the addition of zinc ferrite led to an increase to 100 GΩ cm^2, which remained essentially unchanged after 8 weeks immersion in 3.5 wt% NaCl. The authors explained the improved corrosion resistance by void-filling capability of the inorganic filler, hindering the diffusion of corrosive species toward the coating/metal interface [109].

Polyester is the fourth most-produced polymer, only after polyethylene (PE), polypropylene (PP), and poly(vinyl chloride) (PVC) [111] (Fig. 17.15B). The latter three polymers have also been used as protective coatings. PE and PP are primarily used for packaging (plastic bags, plastic films, bottles), but also the application as anticorrosive coating has been already commercialized. For example, in 2009, METACLAY CJSC launched the manufacture of PE coatings for corrosion protection of steel pipes (e.g., oil pipelines, main gas pipelines,
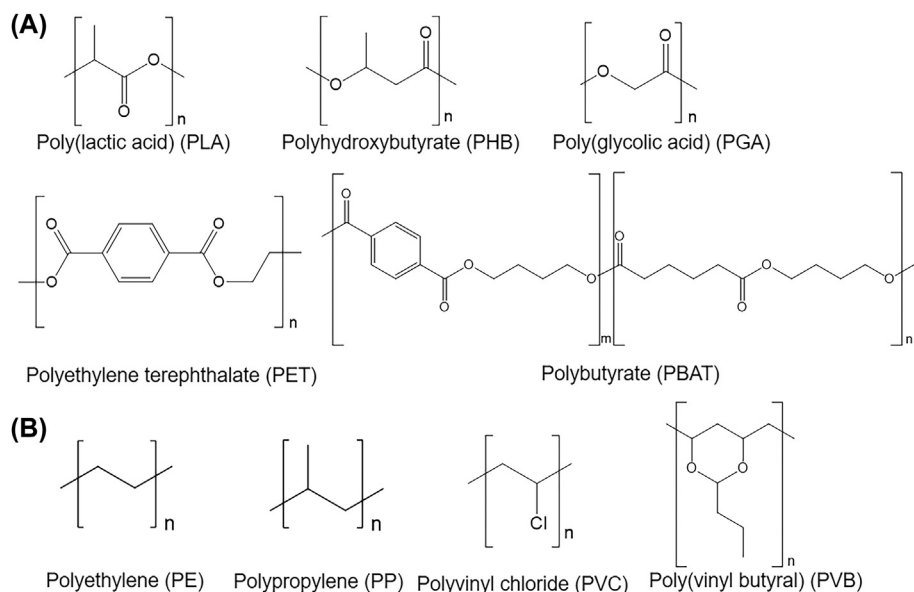
(A)

Poly(lactic acid) (PLA)   Polyhydroxybutyrate (PHB)   Poly(glycolic acid) (PGA)

Polyethylene terephthalate (PET)   Polybutyrate (PBAT)

(B)

Polyethylene (PE)   Polypropylene (PP)   Polyvinyl chloride (PVC)   Poly(vinyl butyral) (PVB)

FIGURE 17.15   Molecular structure of (A) polyesters and (B) other types of polymers.

product pipelines, utility pipelines, etc.). Indeed, PE and PP coatings are extensively used to protect pipelines, mainly in a two- or three-layer design. First the steel pipes are treated by chromate, followed by an epoxy primer ($\sim$150 μm) to promote strong adhesion to the metallic substrate, and then a second layer of 160−200 μm is used to provide compatibility between the epoxy layer and the top coat, which is based on a thick ($\sim$3 mm) PE or PP layer [112−114]. Although two- and three-layer systems have offered excellent results in terms of durable corrosion protection, recent research results indicate that equal or even better performance can be obtained using much thinner layer, as depicted for acrylate, polyurethane, and epoxy-based nanocomposite coatings.

Other less studied polymers and their nanocomposites for corrosion protection application include polystyrene [107], PVB [115], polyetherimide (PEI) [69], among others. One interesting result has been reported by Yang et al. for PVB-fluorographene nanocomposite coating deposited on copper substrate with an impedance modulus of almost 100 GΩ cm^2, essentially unchanged after 90 days in 3.5 wt% NaCl [116].

6. Conclusions

In this chapter, we gave an overview of the recent developments in the field of polymeric nanocomposites applied as coatings for corrosion protection of metallic surfaces. The formulations, synthesis conditions, deposition methods, and properties have been discussed for diverse types of polymeric nanocomposite coatings focusing on their anticorrosive performance. In general, the inclusion of nanofillers into organic matrices results in dense

nanocomposites with elevated barrier property, durability, adhesion to the metallic substrates, thermal stability, mechanical resistance, hydrophobicity, and bioactivity. In particular, organic—inorganic nanocomposites presenting covalent linking between the phases, such as PMMA—silica or epoxy—silica hybrids, show as protective coatings of small thickness ($\sim \mu m$) notable barrier properties, comparable with that of thick paint systems. Furthermore, the inclusion of additives, such as inorganic oxides, clays, carbon nanostructures, and nano- and microcapsules containing organic and inorganic corrosion inhibitors, provide active corrosion protection for the coating, resulting in additional enhancement of their anticorrosive performance. The creative use of nanotechnology has boosted the design of novel protective coatings, based on smart, environmentally friendly, low-cost, and functional polymeric materials.

References

[1] S.V. Harb, A. Trentin, R.F.O. Torrico, S.H. Pulcinelli, C.V. Santilli, P. Hammer, Organic-inorganic hybrid coatings for corrosion protection of metallic surfaces, in: G.C.C. Giudice (Ed.), New Technologies in Protective Coatings, Intech, Rijeka, 2017, pp. 19—51, https://doi.org/10.5772/intechopen.69704.

[2] P. Visser, H. Terryn, J.M.C. Mol, Aerospace coatings, in: A.E. Hughes, J.M.C. Mol, M.L. Zheludkevich, R.G. Buchheit (Eds.), Active Protective Coatings New-Generation Coatings for Metals, Springer Science+Business Media B.V, Dordrecht, 2016, pp. 315—372, https://doi.org/10.1007/978-94-017-7540-3_12.

[3] A.D. Jenkins, P. Kratochvil, R.F.T. Stepto, U.W. Suter, Glossary of basic terms in polymer science, IUPAC 68 (1996) 2287—2311.

[4] T.G. McKenzie, Q. Fu, E.H.H. Wong, D.E. Dunstan, G.G. Qiao, Visible light mediated controlled radical polymerization in the absence of exogenous radical sources or catalysts, Macromolecules 48 (2015) 3864—3872.

[5] K. van Rijswijk, H.E.N. Bersee, Reactive processing of textile fiber-reinforced thermoplastic composites - an overview, Compos. Part A Appl. Sci. Manuf. 38 (2007) 666—681.

[6] C. Duval-Terrié, L. Lebrun, Polymerization and characterization of PMMA, J. Chem. Educ. 2 (2006) 443—446.

[7] P.A. Sorensen, S. Kiil, K. Dam-Johansen, C.E. Weinell, Anticorrosive coatings: a review, J. Coat. Technol. Res. 6 (2009) 135—176.

[8] S.V. Harb, F.C. Dos Santos, B.L. Caetano, S.H. Pulcinelli, C.V. Santilli, P. Hammer, Structural properties of cerium doped siloxane-PMMA hybrid coatings with high anticorrosive performance, RSC Adv. 5 (2015) 15414—15424.

[9] S. Ammar, K. Ramesh, B. Vengadaesvaran, S. Ramesh, A.K. Arof, Formulation and characterization of hybrid polymeric/ZnO nanocomposite coatings with remarkable anti-corrosion and hydrophobic characteristics, J. Coat. Technol. Res. 13 (2016) 921—930.

[10] P. Nguyen-Tri, T.A. Nguyen, P. Carriere, C. Ngo Xuan, Nanocomposite coatings: preparation, characterization, properties, and applications, Int. J. Corros. (2018) 1—19.

[11] C. Sanchez, P. Belleville, M. Popall, L. Nicole, Applications of advanced hybrid organic-inorganic nanomaterials: from laboratory to market, Chem. Soc. Rev. 40 (2011) 696—753.

[12] F.C. Dos Santos, S.V. Harb, M.J. Menu, V. Turq, S.H. Pulcinelli, C.V. Santilli, P. Hammer, On the structure of high performance anticorrosive PMMA-siloxane-silica hybrid coatings, RSC Adv. 5 (2015) 106754—106763.

[13] F. Khelifa, M.E. Druart, Y. Habibi, F. Bénard, P. Leclère, M. Olivier, P. Dubois, Sol-gel incorporation of silica nanofillers for tuning the anti-corrosion protection of acrylate-based coatings, Prog. Org. Coat. 76 (2013) 900—911.

[14] R.B. Figueira, C.J.R. Silva, E.V. Pereira, Organic-inorganic hybrid sol-gel coatings for metal corrosion protection: a review of recent progress, J. Coat. Technol. Res. 12 (2015) 1—35.

[15] P. Hammer, F.C. Dos Santos, B.M. Cerrutti, S.H. Pulcinelli, C.V. Santilli, Highly corrosion resistant siloxane-polymethyl methacrylate hybrid coatings, J. Sol. Gel Sci. Technol. 63 (2012) 266—274.

[16] S. Ammar, K. Ramesh, B. Vengadaesvaran, S. Ramesh, A.K. Arof, A novel coating material that uses nano-sized SiO_2 particles to intensify hydrophobicity and corrosion protection properties, Electrochim. Acta 220 (2016) 417—426.

[17] J. Mosa, N.C. Rosero-Navarro, M. Aparicio, Active corrosion inhibition of mild steel by environmentally-friendly Ce-doped organic-inorganic sol-gel coatings, RSC Adv. 6 (2016) 39577–39586.

[18] M.G. Schiavetto, P. Hammer, C.V. Santilli, S.H. Pulcinelli, F.C. dos Santos, A.V. Benedetti, Improvement of the corrosion resistance of polysiloxane hybrid coatings by cerium doping, J. Non-Cryst. Solids 356 (2010) 2606–2612.

[19] S.V. Harb, B.M. Cerrutti, S.H. Pulcinelli, C.V. Santilli, P. Hammer, Siloxane–PMMA hybrid anti-corrosion coatings reinforced by lignin, Surf. Coat. Technol. 275 (2015) 9–16.

[20] S.V. Harb, S.H. Pulcinelli, C.V. Santilli, K.M. Knowles, P. Hammer, A comparative study on graphene oxide and carbon nanotube reinforcement of PMMA-siloxane-silica anticorrosive coatings, ACS Appl. Mater. Interfaces 8 (2016) 16339–16350.

[21] F. Khelifa, S. Ershov, M.E. Druart, Y. Habibi, D. Chicot, M.G. Olivier, R. Snyders, P. Dubois, A multilayer coating with optimized properties for corrosion protection of Al, J. Mater. Chem. A. 3 (2015) 15977–15985.

[21a] A. Trentin, A.L. Gasparini, F.A. Faria, S.V. Harb, F.C. dos Santos, S.H. Pulcinelli, C.V. Santilli, P. Hammer, Barrier properties of high performance PMMA-silica anticorrosive coatings, Prog. Org. Coat 138 (2020) 105398, https://doi.org/10.1016/j.porgcoat.2019.105398.

[22] K. Hood, Epoxy resins, in: A. Geoffrey, J.C. Bevington (Eds.), Comprehensive Polymer Science and Supplements, Pergamon, 1989, pp. 667–699.

[23] J.J.L. Massingill, R.S. Bauer, Epoxy resins, in: C.D. Craver, C.E. Carraher (Eds.), Applied Polymer Science: 21st Century, Pergamon, 2000, pp. 393–424.

[24] P. He, J. Wang, F. Lu, Q. Ma, Z. Wang, Synergistic effect of polyaniline grafted basalt plates for enhanced corrosion protective performance of epoxy coatings, Prog. Org. Coat. 110 (2017) 1–9.

[25] S. Qiu, C. Chen, W. Zheng, W. Li, H. Zhao, L. Wang, Long-term corrosion protection of mild steel by epoxy coating containing self-doped polyaniline nanofiber, Synth. Met. 229 (2017) 39–46.

[26] B. Ramezanzadeh, G. Bahlakeh, M. Ramezanzadeh, Polyaniline-cerium oxide (PAni-CeO$_2$) coated graphene oxide for enhancement of epoxy coating corrosion protection performance on mild steel, Corros. Sci. 137 (2018) 111–126.

[27] X. Lv, X. Li, N. Li, H. Zhang, Y. zhen Zheng, J. Wu, X. Tao, ZrO$_2$ nanoparticle encapsulation of graphene microsheets for enhancing anticorrosion performance of epoxy coatings, Surf. Coat. Technol. 358 (2019) 443–451.

[28] R.F.A.O. Torrico, S.V. Harb, A. Trentin, M.C. Uvida, S.H. Pulcinelli, C.V. Santilli, P. Hammer, Structure and properties of epoxy-siloxane-silica nanocomposite coatings for corrosion protection, J. Colloid Interface Sci. 513 (2018) 617–628.

[29] S.V. Lamaka, H.B. Xue, N.N.A.H. Meis, A.C.C. Esteves, M.G.S. Ferreira, Fault-tolerant hybrid epoxy-silane coating for corrosion protection of magnesium alloy AZ31, Prog. Org. Coat. 80 (2015) 98–105.

[30] F. Brusciotti, D.V. Snihirova, H. Xue, M.F. Montemor, S.V. Lamaka, M.G.S. Ferreira, Hybrid epoxy-silane coatings for improved corrosion protection of Mg alloy, Corros. Sci. 67 (2013) 82–90.

[31] A. Mahmoodi, M. Ebrahimi, Role of a hybrid dye-clay nano-pigment (DCNP) on corrosion resistance of epoxy coatings, Prog. Org. Coat. 114 (2018) 223–232.

[32] J. Yang, C. Blawert, S.V. Lamaka, D. Snihirova, X. Lu, S. Di, M.L. Zheludkevich, Corrosion protection properties of inhibitor containing hybrid PEO-epoxy coating on magnesium, Corros. Sci. 140 (2018) 99–110.

[33] S. Ammar, K. Ramesh, B. Vengadaesvaran, S. Ramesh, A.K. Arof, Amelioration of anticorrosion and hydrophobic properties of epoxy/PDMS composite coatings containing nano ZnO particles, Prog. Org. Coat. 92 (2016) 54–65.

[34] S. Ammar, K. Ramesh, I.A.W. Ma, Z. Farah, B. Vengadaesvaran, S. Ramesh, A.K. Arof, Studies on SiO$_2$-hybrid polymeric nanocomposite coatings with superior corrosion protection and hydrophobicity, Surf. Coat. Technol. 324 (2017) 536–545.

[35] L.M. Calado, M.G. Taryba, M.J. Carmezim, M.F. Montemor, Self-healing ceria-modified coating for corrosion protection of AZ31 magnesium alloy, Corros. Sci. 142 (2018) 12–21.

[36] Z. Xia, G. Liu, Y. Dong, Y. Zhang, Anticorrosive epoxy coatings based on polydopamine modified molybdenum disulfide, Prog. Org. Coat. 133 (2019) 154–160.

[37] C. Lou, R. Zhang, X. Lu, C. Zhou, Z. Xin, Facile fabrication of epoxy/polybenzoxazine based superhydrophobic coating with enhanced corrosion resistance and high thermal stability, Colloids Surf., A 562 (2019) 8–15.

[38] J. Khodabakhshi, H. Mahdavi, F. Najafi, Investigation of viscoelastic and active corrosion protection properties of inhibitor modified silica nanoparticles/epoxy nanocomposite coatings on carbon steel, Corros. Sci. 147 (2019) 128–140.

IV. Protection of metal using nanocoatings

[39] M. Abdolah Zadeh, S. Van Der Zwaag, S.J. Garcia, Adhesion and long-term barrier restoration of intrinsic self-healing hybrid sol-gel coatings, ACS Appl. Mater. Interfaces 8 (2016) 4126–4136.

[40] I. Díaz, B. Chico, D. De La Fuente, J. Simancas, J.M. Vega, M. Morcillo, Corrosion resistance of new epoxy-siloxane hybrid coatings. A laboratory study, Prog. Org. Coat. 69 (2010) 278–286.

[41] M. Echeverría, C.M. Abreu, K. Lau, C.A. Echeverría, Viability of epoxy-siloxane hybrid coatings for preventing steel corrosion, Prog. Org. Coat. 92 (2016) 29–43.

[42] M. Ganjaee Sari, M. Shamshiri, B. Ramezanzadeh, Fabricating an epoxy composite coating with enhanced corrosion resistance through impregnation of functionalized graphene oxide-co-montmorillonite Nanoplatelet, Corros. Sci. 129 (2017) 38–53.

[43] C. Chen, S. Qiu, M. Cui, S. Qin, G. Yan, H. Zhao, L. Wang, Q. Xue, Achieving high performance corrosion and wear resistant epoxy coatings via incorporation of noncovalent functionalized graphene, Carbon N. Y. 114 (2017) 356–366.

[44] M.H. Wang, Q. Li, X. Li, Y. Liu, L.Z. Fan, Effect of oxygen-containing functional groups in epoxy/reduced graphene oxide composite coatings on corrosion protection and antimicrobial properties, Appl. Surf. Sci. 448 (2018) 351–361.

[45] N.N. Taheri, B. Ramezanzadeh, M. Mahdavian, Application of layer-by-layer assembled graphene oxide nanosheets/polyaniline/zinc cations for construction of an effective epoxy coating anti-corrosion system, J. Alloy. Comp. 800 (2019) 532–549.

[46] C. Li, J. Dai, X. Liu, Y. Jiang, S. Ma, J. Zhu, Green synthesis of a bio-based epoxy curing agent from isosorbide in aqueous condition and shape memory properties investigation of the cured resin, Macromol. Chem. Phys. 217 (2016) 1439–1447.

[47] E. Koh, S. Lee, J. Shin, Y.W. Kim, Renewable polyurethane microcapsules with isosorbide derivatives for self-healing anticorrosion coatings, Ind. Eng. Chem. Res. 52 (2013) 15541–15548.

[48] D. Akram, E. Sharmin, S. Ahmad, Linseed polyurethane/tetraethoxyorthosilane/fumed silica hybrid nanocomposite coatings: physico-mechanical and potentiodynamic polarization measurements studies, Prog. Org. Coat. 77 (2014) 957–964.

[49] D. Akram, O. Hakami, E. Sharmin, S. Ahmad, Castor and linseed oil polyurethane/TEOS hybrids as protective coatings: a synergistic approach utilising plant oil polyols, a sustainable resource, Prog. Org. Coat. 108 (2017) 1–14.

[50] S. Pathan, S. Ahmad, Green and sustainable anticorrosive coating derived from waterborne linseed alkyd using organic-inorganic hybrid cross linker, Prog. Org. Coat. 122 (2018) 189–198.

[51] J. Konieczny, K. Loos, Green polyurethanes from renewable isocyanates and biobased white dextrins, Polymers 11 (2019) 1–10.

[52] D.K. Chattopadhyay, K.V.S.N. Raju, Structural engineering of polyurethane coatings for high performance applications, Prog. Polym. Sci. 32 (2007) 352–418.

[53] M.C.L. de Oliveira, R.A. Antunes, I. Costa, Effect of the NCO/OH molar ratio on the physical aging and on the electrochemical behavior of polyurethane-urea hybrid coatings, Int. J. Electrochem. Sci. 8 (2013) 4679–4689.

[54] S. Ahmad, F. Zafar, E. Sharmin, N. Garg, M. Kashif, Synthesis and characterization of corrosion protective polyurethane fattyamide/silica hybrid coating material, Prog. Org. Coat. 73 (2012) 112–117.

[55] E. Maya-Visuet, T. Gao, M. Soucek, H. Castaneda, The effect of TiO_2 as a pigment in a polyurethane/polysiloxane hybrid coating/aluminum interface based on damage evolution, Prog. Org. Coat. 83 (2015) 36–46.

[56] D. Del Angel-López, M.A. Domínguez-Crespo, A.M. Torres-Huerta, A. Flores-Vela, J. Andraca-Adame, H. Dorantes-Rosales, Analysis of degradation process during the incorporation of ZrO_2:SiO_2 ceramic nanostructures into polyurethane coatings for the corrosion protection of carbon steel, J. Mater. Sci. 48 (2013) 1067–1084.

[57] Y. Ahmadi, S. Ahmad, Surface-active antimicrobial and anticorrosive Oleo-Polyurethane/graphene oxide nanocomposite coatings: synergistic effects of in-situ polymerization and π-π interaction, Prog. Org. Coat. 127 (2019) 168–180.

[58] H. Khatoon, S. Ahmad, Vanadium pentoxide-enwrapped polydiphenylamine/polyurethane nanocomposite: high-performance anticorrosive coating, ACS Appl. Mater. Interfaces 11 (2019) 2374–2385.

[59] A. Ghosal, O.U. Rahman, S. Ahmad, High-performance soya polyurethane networked silica hybrid nanocomposite coatings, Ind. Eng. Chem. Res. 54 (2015) 12770–12787.

[60] A.C. Ferrel-álvarez, M.A. Domínguez-Crespo, A.M. Torres-Huerta, H. Cong, S.B. Brachetti-Sibaja, A.B. López-Oyama, Intensification of electrochemical performance of AA7075 aluminum alloys using rare earth functionalized water-based polymer coatings, Polymers 9 (2017) 1–23.

IV. Protection of metal using nanocoatings

[61] A.M. Kumar, M.M. Rahman, Z.M. Gasem, A promising nanocomposite from CNTs and nano-ceria: nanostructured fillers in polyurethane coatings for surface protection, RSC Adv. 5 (2015) 63537−63544.

[62] E.C. Romani, S. Nardecchia, C. Vilani, S. Qi, H. Dong, F.L. Freire, Synthesis and characterization of polyurethane/reduced graphene oxide composite deposited on steel, J. Coat. Technol. Res. 15 (2018) 1371−1377.

[63] J. Sun, H. Fang, H. Wang, S. Yang, S. Xiao, Y. Ding, Waterborne epoxy-modified polyurethane-acrylate dispersions with nano-sized core-shell structure particles: synthesis, characterization, and their coating film properties, J. Polym. Eng. 37 (2016) 113−123.

[64] X. Ye, Z. Wang, L. Ma, Q. Wang, A. Chu, Zinc oxide array/polyurethane nanocomposite coating: fabrication, characterization and corrosion resistance, Surf. Coat. Technol. 358 (2019) 497−504.

[65] S. Ashhari, A.A. Sarabi, S.M. Kasiriha, D. Zaarei, Aliphatic polyurethane-montmorillonite nanocomposite coatings: preparation, characterization, and anticorrosive properties, J. Appl. Polym. Sci. 119 (2011) 523−529.

[66] F. Lu, B. Song, J. Wang, Preparation and characterization of acrylic polyurethane/polyaniline nanocomposite coatings, Int. J. Electrochem. Sci. 12 (2017) 2679−2691.

[67] C.Y. Huang, P.Y. Tsai, B.E. Gu, W. Hu, J.S. Jhao, G.S. Jhaung, Y.L. Lee, The development of novel sound-absorbing and anti-corrosion composite coating, ECS Trans. 72 (2016) 171−183.

[68] B.E. Gu, C.Y. Huang, T.H. Shen, Y.L. Lee, Effects of multiwall carbon nanotube addition on the corrosion resistance and underwater acoustic absorption properties of polyurethane coatings, Prog. Org. Coat. 121 (2018) 226−235.

[69] A. Zomorodian, M.P. Garcia, T. Moura e Silva, J.C.S. Fernandes, M.H. Fernandes, M.F. Montemor, Corrosion resistance of a composite polymeric coating applied on biodegradable AZ31 magnesium alloy, Acta Biomater. 9 (2013) 8660−8670.

[70] A. Lutz, O. van den Berg, J. Wielant, I. De Graeve, H. Terryn, A multiple-action self-healing coating, Front. Mater. 2 (2016) 1−12.

[71] L.W. McKeen, Fluoropolymers, in: L.W. McKeen (Ed.), Fatigue and Tribological Properties of Plastics and Elastomers, second ed., William Andrew Publishing, 2010, pp. 249−264.

[72] A.S. Hamdy, Fluoropolymer coatings for corrosion protection in highly aggressive environments, in: A.S. Khanna (Ed.), High-Performance Organic Coatings, Woodhead, 2008, pp. 212−224.

[73] A.S. Hamdy, A.M. Beccaria, T. Temtchenko, Corrosion protection of AA6061 T6 by fluoropolymer coatings in NaCl solution, Surf. Coat. Technol. 155 (2002) 176−183.

[74] F. Deflorian, L. Fedrizzi, P.L. Bonora, Impedance study of the corrosion protection properties of fluoropolymer coatings, Prog. Org. Coat. 23 (1993) 73−88.

[75] F. Deflorian, L. Fedrizzi, D. Lenti, P.L. Bonora, On the corrosion protection properties of fluoropolymer coatings, Prog. Org. Coat. 22 (1993) 39−53.

[76] S.V. Gnedenkov, S.L. Sinebryukhov, D.V. Mashtalyar, K.V. Nadaraia, A.S. Gnedenkov, V.M. Bouznik, Composite fluoropolymer coatings on the MA8 magnesium alloy surface, Corros. Sci. 111 (2016) 175−185.

[77] F. Deflorian, L. Fedrizzi, A. Locaspi, P.L. Bonora, Testing of corrosion resistant fluoropolymer coatings, Electrochim. Acta 38 (1993) 1945−1950.

[78] T.F. da Conceicao, N. Scharnagl, W. Dietzel, D. Hoeche, K.U. Kainer, Study on the interface of PVDF coatings and HF-treated AZ31 magnesium alloy: determination of interfacial interactions and reactions with self-healing properties, Corros. Sci. 53 (2011) 712−719.

[79] M. Mihelčič, M. Gaberšček, M. Salzano de Luna, M. Lavorgna, C. Giuliani, G. Di Carlo, A.K. Surca, Effect of silsesquioxane addition on the protective performance of fluoropolymer coatings for bronze surfaces, Mater. Des. 178 (2019) 1−13.

[80] D.W. DeBerry, Modification of the electrochemical and corrosion behavior of stainless steels with an electroactive coating, J. Electrochem. Soc. 132 (2006) 1022−1026.

[81] N.R. Tanguy, M. Thompson, N. Yan, A review on advances in application of polyaniline for ammonia detection, Sens. Actuators B Chem. 257 (2018) 1044−1064.

[82] J. Stejskal, R.G. Gilbert, Polyaniline. Preparation of a conducting polymer, Pure Appl. Chem. 74 (2002) 857−867.

[83] Y. Zhang, Y. Shao, X. Liu, C. Shi, Y. Wang, G. Meng, X. Zeng, Y. Yang, A study on corrosion protection of different polyaniline coatings for mild steel, Prog. Org. Coat. 111 (2017) 240−247.

[84] P.P. Deshpande, N.G. Jadhav, V.J. Gelling, D. Sazou, Conducting polymers for corrosion protection: a review, J. Coat. Technol. Res. 11 (2014) 473−494.

[85] A.A. Salem, B.N. Grgur, The influence of the polyaniline initial oxidation states on the corrosion of steel with composite coatings, Prog. Org. Coat. 119 (2018) 138−144.

[86] T.-H. Kuo, C.-J. Weng, C.-L. Chen, Y.-L. Chen, C.-H. Chang, J.-M. Yeh, Electrochemical investigations on the corrosion protection effect of poly(vinyl carbazole)-silica hybrid sol-gel materials, Polym. Polym. Compos. 33 (2012) 275−281.

[87] M. Ates, A review on conducting polymer coatings for corrosion protection, J. Adhes. Sci. Technol. 30 (2016) 1510−1536.

[88] M. Ates, A. Dolapdere, Poly(3-Octylthiophene) and poly(3-Octylthiophene)/TiO_2-coated on Al1050: electrosynthesis, characterization and its corrosion protection ability in NaCl solution, Polym. Plast. Technol. Eng. 53 (2014) 1768−1777.

[89] N.C.T. Martins, T. Moura e Silva, M.F. Montemor, J.C.S. Fernandes, M.G.S. Ferreira, Polyaniline coatings on aluminium alloy 6061-T6: electrosynthesis and characterization, Electrochim. Acta 55 (2010) 3580−3588.

[90] N.C.T. Martins, T. Moura e Silva, M.F. Montemor, J.C.S. Fernandes, M.G.S. Ferreira, Electrodeposition and characterization of polypyrrole films on aluminium alloy 6061-T6, Electrochim. Acta 53 (2008) 4754−4763.

[91] B.N. Grgur, A.R. Elkais, M.M. Gvozdenović, S. Drmanić, T.L. Trišović, B.Z. Jugović, Corrosion of mild steel with composite polyaniline coatings using different formulations, Prog. Org. Coat. 79 (2015) 17−24.

[92] M. Shabani-Nooshabadi, S.M. Ghoreishi, M. Behpour, Direct electrosynthesis of polyaniline-montmorrilonite nanocomposite coatings on aluminum alloy 3004 and their corrosion protection performance, Corros. Sci. 53 (2011) 3035−3042.

[93] K.C. Chang, G.W. Jang, C.W. Peng, C.Y. Lin, J.C. Shieh, J.M. Yeh, J.C. Yang, W.T. Li, Comparatively electrochemical studies at different operational temperatures for the effect of nanoclay platelets on the anticorrosion efficiency of DBSA-doped polyaniline/Na^+-MMT clay nanocomposite coatings, Electrochim. Acta 52 (2007) 5191−5200.

[94] A.T. Gokçeoren, C. Erbil, Morphological characterization and electrochemical/electrical properties of poly(N-vinyl carbazole)/montmorillonite composites, Polym. Polym. Compos. 32 (2011) 1325−1335.

[95] M. Ates, E. Topkaya, Nanocomposite film formations of polyaniline via TiO_2, Ag, and Zn, and their corrosion protection properties, Prog. Org. Coat. 82 (2015) 33−40.

[96] M. Ates, O. Kalender, E. Topkaya, L. Kamer, Polyaniline and polypyrrole/TiO_2 nanocomposite coatings on Al1050: electrosynthesis, characterization and their corrosion protection ability in saltwater media, Iran, Polym. J. 24 (2015) 607−619.

[97] M.F. Amirdehi, D. Afzali, Deposition of polyaniline/silica nanocomposite coating on stainless steel; study of its corrosion properties, Adv. Mater. Res. 829 (2014) 605−609.

[98] C.-H. Chang, T.-C. Huang, C.-W. Peng, T.-C. Yeh, H.-I. Lu, W.-I. Hung, C.-J. Weng, T.-I. Yang, J.-M. Yeh, Novel anticorrosion coatings prepared from polyaniline/graphene composites, Carbon N. Y. 50 (2012) 5044−5051.

[99] L. Jiang, J.A. Syed, H. Lu, X. Meng, In-situ electrodeposition of conductive polypyrrole-graphene oxide composite coating for corrosion protection of 304SS bipolar plates, J. Alloy. Comp. 770 (2019) 35−47.

[100] A. Madhan Kumar, Z.M. Gasem, Effect of functionalization of carbon nanotubes on mechanical and electrochemical behavior of polyaniline nanocomposite coatings, Surf. Coat. Technol. 276 (2015) 416−423.

[101] A. Davoodi, S. Honarbakhsh, G.A. Farzi, Evaluation of corrosion resistance of polypyrrole/functionalized multi-walled carbon nanotubes composite coatings on 60Cu-40Zn brass alloy, Prog. Org. Coat. 88 (2015) 106−115.

[102] F.B. Diniz, G.F. De Andrade, C.R. Martins, W.M. De Azevedo, A comparative study of epoxy and polyurethane based coatings containing polyaniline-DBSA pigments for corrosion protection on mild steel, Prog. Org. Coat. 76 (2013) 912−916.

[103] P.T. Bertuoli, A.F. Baldissera, A.J. Zattera, C.A. Ferreira, C. Alemán, E. Armelin, Polyaniline coated core-shell polyacrylates: control of film formation and coating application for corrosion protection, Prog. Org. Coat. 128 (2019) 40−51.

[104] W. Sun, L. Wang, T. Wu, Y. Pan, G. Liu, Synthesis of low-electrical-conductivity graphene/pernigraniline composites and their application in corrosion protection, Carbon N. Y. 79 (2014) 605−614.

[105] S.S. Pathak, A.S. Khanna, Investigation of anti-corrosion behavior of waterborne organosilane-polyester coatings for AA6011 aluminum alloy, Prog. Org. Coat. 65 (2009) 288−294.

[106] G. Verma, S.K. Dhoke, A.S. Khanna, Polyester based-siloxane modified waterborne anticorrosive hydrophobic coating on copper, Surf. Coat. Technol. 212 (2012) 101−108.

[107] Y.H. Yu, Y.Y. Lin, C.H. Lin, C.C. Chan, Y.C. Huang, High-performance polystyrene/graphene-based nanocomposites with excellent anti-corrosion properties, Polym. Chem. 5 (2014) 535−550.

[108] A. Golgoon, M. Aliofkhazraei, M. Toorani, M.H. Moradi, A.S. Rouhaghdam, Corrosion and wear properties of nanoclay- polyester nanocomposite coatings fabricated by electrostatic method, Procedia Mater. Sci. 11 (2015) 536−541.

[109] S. Mahvidi, M. Gharagozlou, M. Mahdavian, S. Naghib, Anticorrosive performance of polyester-melamine coating fortified with zinc ferrite nanoparticles, Prog. Color. Color. Coat. 12 (2019) 57−70.

[110] M.H. Moradi, A. Golgoon, M. Aliofkhazraei, A. Sabour Rouhaghdam, M. Asgari, M. Toorani, Corrosion behavior of ZnO-polyester nanocomposite powder coating, Anti-Corrosion Methods Mater. 64 (2017) 380−388.

[111] M.W. Allsopp, G. Vianello, Poly(Vinyl chloride), Ullmann's Encycl. Ind. Chem. 28 (2012) 441−468.

[112] A. Samimi, S. Zarinabadi, An analysis of polyethylene coating corrosion in oil and gas pipelines, J. Am. Sci. 7 (2011) 1032−1036.

[113] J.N. Murray, P.J. Moran, ElS study of the corrosion behavior of polyethylene coating holidays in natural soil conditions, Corrosion 45 (1989) 885−895.

[114] G.P. Guidetti, G.L. Rigosi, R. Marzola, The use of polypropylene in pipeline coatings, Prog. Org. Coat. 27 (1996) 79−85.

[115] C.F. Glover, C. Richards, J. Baker, G. Williams, H.N. McMurray, In-coating graphene nano-platelets for environmentally-friendly corrosion protection of iron, Corros. Sci. 114 (2017) 169−172.

[116] Z. Yang, W. Sun, L. Wang, S. Li, T. Zhu, G. Liu, Liquid-phase exfoliated fluorographene as a two dimensional coating filler for enhanced corrosion protection performance, Corros. Sci. 103 (2016) 312−318.